Early- and life-long intake of dietary advanced glycation end-products (dAGEs) leads to transient tissue accumulation, increased gut sensitivity to inflammation, and slight changes in gut microbial diversity, without causing overt disease

M.T. Nogueira Silva Lima, C. Delayre-Orthez, M. Howsam, P. Jacolot, C. Niquet-Léridon, A. Okwieka, P.M. Anton, M. Perot, N. Barbezier, H. Mathieu, et al.

Food Research International 195 (2024) 114967

Contents lists available at ScienceDirect

Food Research International

journal homepage: www.elsevier.com/locate/foodres

Early- and life-long intake of dietary advanced glycation end-products (dAGEs) leads to transient tissue accumulation, increased gut sensitivity to inflammation, and slight changes in gut microbial diversity, without causing overt disease

M.T. Nogueira Silva Lima [a], C. Delayre-Orthez [b], M. Howsam [a], P. Jacolot [b], C. Niquet-Léridon [b], A. Okwieka [c], P.M. Anton [b], M. Perot [b], N. Barbezier [b], H. Mathieu [b], A. Ghinet [a,e], C. Fradin [a], E. Boulanger [a], S. Jaisson [c,d], P. Gillery [c,d], F.J. Tessier [a,*]

[a] U1167-RID-AGE-Facteurs de Risque et Déterminants Moléculaires des Maladies Liées au Vieillissement, Institut Pasteur de Lille, University Lille, Inserm, CHU Lille, F-59000 Lille, France
[b] Institut Polytechnique UniLaSalle, Université d'Artois, ULR 7519, Equipe PETALES, 60000 Beauvais, France
[c] University of Reims Champagne-Ardenne, Laboratory of Biochemistry and Molecular Biology, CNRS/URCA UMR 7369 MEDyC, Faculté de Médecine, 51095 Reims, France
[d] University Hospital of Reims, Laboratory of Biochemistry-Pharmacology-Toxicology, 51092 Reims, France
[e] Junia, Health and Environment, Laboratory of Sustainable Chemistry and Health, 59000 Lille, France

ARTICLE INFO

Keywords:
Glycation
Carboxymethyl-lysine
RAGE
Inflammation
Senescence
Oxidative stress
Microbiota

ABSTRACT

Dietary advanced glycation end-products (dAGEs) accumulate in organs and are thought to initiate chronic low-grade inflammation (CLGI), induce glycoxidative stress, drive immunosenescence, and influence gut microbiota. Part of the toxicological interest in glycation products such as dietary carboxymethyl-lysine (dCML) relies on their interaction with receptor for advanced glycation end-products (RAGE). It remains uncertain whether early or lifelong exposure to dAGEs contributes physiological changes and whether such effects are reversible or permanent. Our objective was to examine the physiological changes in Wild-Type (WT) and RAGE KO mice that were fed either a standard diet (STD − 20.8 ± 5.1 μg dCML/g) or a diet enriched with dCML (255.2 ± 44.5 μg dCML/g) from the perinatal period for up to 70 weeks. Additionally, an early age (6 weeks) diet switch (dCML→STD) was explored to determine whether potential harmful effects of dCML could be reversed. Previous dCML accumulation patterns described by our group were confirmed here, with significant RAGE-independent accumulation of dCML in kidneys, ileum and colon over the 70-week dietary intervention (respectively 3-fold, 17-fold and 20-fold increases compared with controls). Diet switching returned tissue dCML concentrations to their baseline levels. The dCML-enriched diet had no significative effect on endogenous glycation, inflammation, oxidative stress or senescence parameters. The relative expression of *TNFα*, *VCAM1*, *IL6*, and *P16* genes were all upregulated (~2-fold) in an age-dependent manner, most notably in the kidneys of WT animals. RAGE knockout seemed protective in this regard, diminishing age-related renal expression of *TNFα*. Significant increases in *TNFα* expression were detectable in the intestinal tract of the Switch group (~2-fold), suggesting a higher sensitivity to inflammation perhaps related to the timing of the diet change. Minor fluctuations were observed at family level within the caecal microbiota, including Eggerthellaceae, Anaerovoracaceae and Marinifilaceae communities, indicating slight changes in composition. Despite chronic dCML consumption resulting in higher free CML levels in tissues, there were no substantial increases in parameters related to inflammageing. Age was a more important factor in inflammation status, notably in the kidneys, while the early-life dietary switch may have influenced intestinal susceptibility to inflammation. This study affirms the therapeutic potential of RAGE modulation and corroborates evidence for the disruptive effect of dietary changes occurring too early in life. Future research

Abbreviations: AGEs, dietary advanced glycation end-products; CEL, Carboxyethyl-lysine; CLGI, chronic low-grade inflammation; CML, carboxymethyl-lysine; IQR, Interquartile range; MG-H1, Methylglyoxal-derived hydroimidazolone; RAGE, receptor for advanced glycation end-products; WT, Wild-Type.

* Corresponding author.
E-mail address: frederic.tessier@univ-lille.fr (F.J. Tessier).

https://doi.org/10.1016/j.foodres.2024.114967
Received 23 May 2024; Received in revised form 13 August 2024; Accepted 20 August 2024
Available online 23 August 2024

should prioritize the potential influence of dAGEs on disease aetiology and development, notably any exacerbating effects they may have upon existing health conditions.

1. Introduction

Human life expectancy has increased in recent decades (WHO, 2023), bringing ageing to the fore as a topic of interest for researchers and policy makers. Ageing is a multifactorial process influenced by intrinsic (*e.g.* individual genome, metabolism), and environmental (*e.g.* diet, smoking) factors (Melzer et al., 2020). The presence of persistent, chronic low-grade inflammation (CLGI) over a person's lifespan, resulting in increased oxidative stress processes, plays a fundamental role in the development of age-related changes in physiological functions, and is commonly referred to as "inflammageing" (Sanada et al., 2018; Zuo et al., 2019). Diet is often cited as having the potential for both positive and negative effects upon a person's health. Diet may not only influence quality of life in adulthood, but is also considered to have a major influence on health in early life, including the intrauterine period (Dawson et al., 2021; Dunkerton & Aiken, 2022). Parental eating behaviour has been demonstrated to reprogram children's epigenome, having permanent neurobiological effects and increasing susceptibility to obesity and diabetes (Bodden et al., 2020; Chen et al., 2016). These findings suggest that this period of life is one in which genomic, metabolic, immunological and gut microbiota reprogramming may take place (Bodden et al., 2020; Fetissov & Hökfelt, 2019; Tamashiro & Moran, 2010).

The harmful effects of diet are thought to be partly linked to the presence in food of contaminants, such as pesticides, and neoformed compounds resulting from transformation of ingredients (Margină et al., 2020). Among the latter is a group of chemically diverse molecules called Advanced Glycation End-Products (AGEs), which originates from the non-enzymatic reaction between amino acids and reactive sugars (Rabbani & Thornalley, 2018). Lysine moieties are major glycation targets leading to the formation of diverse AGEs such as N^{ε}-carboxymethyl-lysine (CML), a stable biomarker of endogenous and exogenous glycation (Tessier et al., 2021). Glycation happens both *in vivo* under physiological conditions (endogenous glycation), and in foods during processing or storage (exogenous glycation) (van Dongen et al., 2022).

Dietary CML (dCML) in food exists predominantly in protein-bound form, and has been reported as having affinity for RAGE, the receptor for AGEs (van Dongen et al., 2021; Xue et al., 2014). RAGE is a transmembrane receptor, with multiple ligands other than the AGEs that gave it its name, that is involved in cellular survival responses (Rojas et al., 2022). It is expressed in multiple immune cell types, which may include T lymphocytes such as CD4 + cells, in which it participates in the regulation of adaptive immunity (Teissier et al., 2022). Dietary AGEs (dAGEs) are quite widely studied, and the quantity to which people are exposed through dietary sources is reasonably well characterised. Several foods such as bread, cookies and milk (including infant formulae) have elevated levels of dCML. RAGE, which plays a role in downstream activation of inflammation, is suggested to partially mediate the impact of AGEs on CLGI, oxidative stress activation and subsequent accelerated ageing (Frimat et al., 2019). While no consensus yet exists, circulatory dAGEs and their accumulation in tissues are nevertheless considered to be potential triggers of inflammation, oxidative stress, immunosenescence and cellular aging (Nogueira Silva Lima et al., 2021).

With these main concepts and recent scientific discoveries in mind, we hypothesised that exposure to dCML (in early life and/or throughout life) participates in the establishment of CLGI and a pro-oxidative status by a mechanism mediated by the AGE-RAGE axis. We further hypothesised that the absence of RAGE would play a protective role in genetically modified RAGE-knockout mice (RAGE KO). In addition, the consumption of dCML has been shown to result in accumulation of dCML in tissues (Tessier et al., 2016), thereby increasing oxidative stress, accelerating immunosenescence and remodelling gut microbiota. To examine the reversibility of the effects of dCML exposure, we hypothesised that an early-life switch to a lower level of dCML could attenuate or reverse these putative long-term, deleterious effects, as recently reported in young healthy mice (van Dongen et al., 2021). Our goal was to address the early-life and life-long effects of chronic consumption of dCML over inflammation, oxidative stress, immunosenescence, gut microbiota homeostasis, and the accumulation of free and protein-bound CML in 6, 35, and 70-week-old Wild-Type (WT) and RAGE KO C57BL/6 mice in a crossover feeding trial beginning the perinatal period.

2. Materials and methods

2.1. In vivo experiments

2.1.1. Animals

Male and female C57BL/6 mice were housed under controlled temperature (20 °C) and 12 h light–dark cycles, with free access to food and water throughout the study. Experiments conducted at the EOPS1 Animal Facility, University of Lille (France), in compliance with local ethical procedures and approval under the protocol APAFIS 23208–2019120215543800 v4 (ANR ExoAgeing). Inbred WT and RAGE KO (University of Heidelberg, Germany (Constien et al., 2001)) were used as models. Animals were generated from the crossing of heterozygous founder animals (1st Generation – F1). From the resulting offspring, only homozygous WT or RAGE KO were selected ensuring the same genetic background within each strain. Littermates were then crossed (2nd generation – F2) to generate the offspring used in dietary experiments.

2.1.2. Diet

Previous work by our group has shown that the overwhelming majority of free CML in the body is directly related to dietary intake of dCML (Tessier et al., 2016). For this reason, we have occasionally employed the terms "free CML" and "dCML" interchangeably in the following sections. To test the effects of dCML consumption, two different diets were prepared by SAFE Diets (Augy, France): a Standard Diet (STD) enriched with non-glycated bovine serum albumin (BSA), and dCML Diet (dCML) enriched with dCML-BSA, by modifying the normal rodent regimes (A03 and A04). Both food formulas were enriched with the addition of glycated or non-glycated BSA. A complete description and characterization of the synthesis of glycated BSA used in the current study has recently been published elsewhere (Nogueira Silva Lima et al., 2023). The A03 diet was provided during breeding and maternal feeding periods (21 % protein), while the A04 diets were provided from weaning and throughout adult life (16 % of protein) (Fig. 1).

Average dCML amounts quantified by LC-MS/MS were 20.8 ± 5.0 μg dCML/g Dry Weight (DW) food in the STD diet and 255.2 ± 44.0 μg dCML/g DW food in the dCML-enriched diet. An equivalent proportion of BSA, either untreated or glycated, was used to modify both diets so there was no difference in protein content between them. Final protein addition did not exceed 0.8 % of the total protein provided to the animals. Nutritional quality (lysine and total protein levels), as well as dCML and furosine amounts, were measured across the different batches to verify homogeneity and consistency of mice pellet preparation (Nogueira Silva Lima et al., 2023).

2.1.3. Experimental design

The experimental design is graphically represented in Fig. 1. For testing the lifelong effects of dCML exposure, WT and RAGE KO mice were divided into two groups fed with either STD or dCML diets. To test the reversibility of the effects of early-life consumption of dCML, a third "Switch" group of WT animals underwent a diet change at 6 weeks old from the dCML to the STD diet. Animals were randomly allocated to the different treatments (see Table 3). Food intake data was recorded over a one-week period in 63-week-old (on average) animals.

2.1.4. Collection of tissues and fluids

Sacrifices proceeded after the injection of ketamine/xylazine (150 mg/kg:10 mg/kg) followed by cervical dislocation. After 6, 35, and 70 weeks of dietary intervention animals were sacrificed, and the kidneys, skin, ileum, colon, plasma (obtained from heparinized blood by centrifugation at 2,000 g for 10 min), spleen and caecum were collected to evaluate glycation, inflammation, immunosenescence, and metagenomic associated parameters. For the Switch group, animals were sacrificed, and organs collected after 35 and 70 weeks of diet. Samples were immediately preserved in liquid nitrogen and then stored at −80 °C until analysis. Each sample was treated appropriately for the experiments described in Table 1.

Table 1
Biomarker panel for the evaluation of CLGI and its crosstalking factors in the murine model.

Parameter	Target	Biomarker	Technique
Glycation	Kidneys, skin, ileum, colon, plasma	Free and protein-bound CML	LC/MS-MS
Oxidative stress	Plasma, Ileum, Colon	MDA, protein carbonylation, *SOD1/2*, MPO	Colorimetrics, RT-qPCR
Inflammation	Kidneys, ileum, colon	*GLO1, IL-6, TNFα, VCAM-1, RAGE, SIRT1, P16, GLβ1, PGC1α*	RT-qPCR
Lymphocyte orientation and inflammation	Spleen	*SIRT1, P16, GLβ1, TBox21, GATA 3, FOXp3, RORγT*	RT-qPCR
Microbiota	Caecum	Microbial diversity	16S Metagenomics

2.2. Quantification of free and protein-bound CML

2.2.1. Chemical and reagents

All reagents used were analytical grade. Ultra-pure HPLC water and Ammonium formate (>99 %) were from VWR (Fontenay-sous-Bois, France). Acetonitrile (ACN), boric acid (H_3BO_3), formic acid (>95 %), hydrochloric acid (HCl) 37 %, sodium hydroxide (NaOH), trichloroacetic acid (TCA), nonafluoropentanoic acid (NFPA) 97 % and lysine (Lys), were all obtained from Sigma–Aldrich (Saint-Quentin-Fallavier, France). The dCML and dCML-d_2 standards were from Iris Biotech (Marktredwitz, Germany). Labelled Lys-d8 and Lys-$^{15}N_2$ were from CDN Isotopes (Toronto, Canada) and CortecNet (Voisins-le-Bretonneux, France), respectively.

2.2.2. Quantification of free and protein-bound CML by mass spectrometry

Free CML was measured in all samples, and protein-bound CML was measured in plasma, kidneys, and skin according to the methodology described by (Helou et al., 2022) with modifications.

2.2.2.1. Sample preparation for the quantification of free and protein-bound CML in plasma. Free CML was determined in the supernatant after precipitating proteins in the sample. Lysine was measured simultaneously with dCML in the protein fractions. Quantification of dCML and lysine was performed by isotope dilution using liquid chromatography with tandem mass spectrometry detection (LC-MS/MS) in all cases.

For plasma samples, 30 μL plasma were transferred to a 2 mL, screw-top polypropylene (PP) tube to which 30 μL of 20 % TCA were added. This was mixed with a vortex mixer and then left on ice for 30 min before centrifuging at 20,000 g for 5 min at 4 °C. The supernatant was aspirated (40 μL for all samples) and evaporated to dryness in a Speed-vac apparatus (ThermoFisher). Just before analysis, the dried supernatant was resolubilized in the HPLC mobile phase with dCML-d_2 internal standard.

The protein pellet remaining in the 2 mL PP tube after removal of the supernatant was then reduced with 600 μL of 0.1 M $NaBH_4$ for 2 h at room temperature. At the end of this time, 600 μL of 12 M HCl were added, and the sample hydrolysed at 110 °C for 18 h, after which the

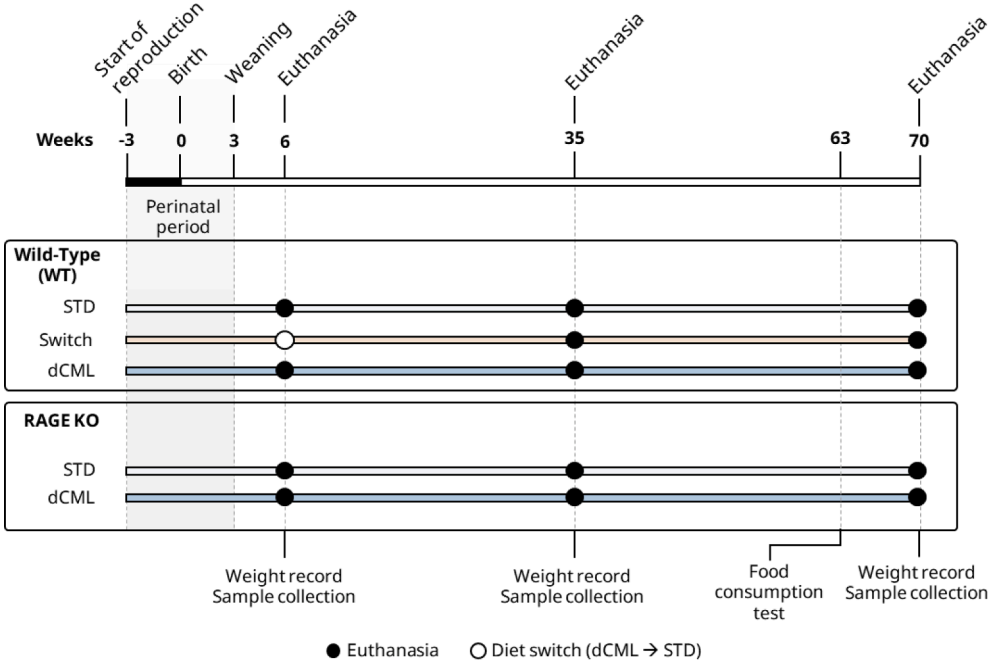

Fig. 1. Schematic representation of the experimental design.

tubes were centrifuged once more (15,000 g, 5 min at 4 °C) before 1 mL of supernatant was aspirated and evaporated to dryness under nitrogen. One millilitre of water was added, and the sample again evaporated to dryness, in order to remove as much residual HCl as possible, before being resolubilised in the HPLC mobile phase with dCML-d_2 internal standard, centrifuged (15000 g, 5 min at 4 °C), then filtered into HPLC vials (Uptidisc PTFE, 0.45 μm).

2.2.2.2. Sample preparation for the quantification of dCML in kidneys, skin, ileum and colon, and protein-bound CML in kidneys and skin. This study is the result of a collaborative project in which two different laboratories shared the analysis of CML in plasma and organs, hence the two different analytical methods on colon and ileum samples analysed by the ULR 7519 at the UniLaSalle Beauvais and plasma, kidneys, and skin analysed by the UMR 7369 University of Reims are described below.

Free CML was determined by direct measurement in the supernatant after precipitating proteins in all samples. Twenty-five to 80 mg of tissue were homogenized in a bead mill (FastPrep24, FischerSci) with 800 μL ultrapure water (4x 40 s cycles at 6 m/s). The tube was centrifuged (15,000 g, 5 min at 4 °C) and 200 μL of supernatant were transferred to a 2 mL, screw-top PP tube. Fifty microliters of TCA (50 %) were added, mixed with a vortex mixer, then the tube was left on ice for 30 min before centrifuging at 20,000 g for 5 min at 4 °C. The supernatant was aspirated (180 μL for all samples) and evaporated to dryness in a SpeedVac. Just before analysis, the dried supernatant was resolubilised in the HPLC mobile phase with CML-d_2 and lysine-d_8 / lysine-$^{15}N_2$ internal standards.

For samples of kidneys and skin, 600 μL of 0.1 M $NaBH_4$ were added to the protein pellet remaining in the 2 mL PP tube, and the tube was left for 2 h at room temperature. Then 600 μL of 12 M HCl were added, and the sample hydrolysed at 110 °C for 18 h. Tubes were centrifuged once more (15,000 g, 5 min at 4 °C) before 1 mL of supernatant was aspirated and evaporated to dryness under nitrogen. One millilitre of water was added, and the sample again evaporated to dryness to remove as much residual HCl as possible, before the sample was resolubilized in the HPLC mobile phase with dCML-d_2 and lysine-d_8 / lysine-$^{15}N_2$ internal standards, centrifuged (15000 g, 5 min at 4 °C), then filtered into HPLC vials (UPTIDISC PTFE, 0,45 μm).

2.2.2.3. Quantification of CML by LC-MS/MS in kidneys, skin, ileum, colon, and plasma by LC-MS/MS. Hydrolysed sample preparations of plasma, kidneys and skin were separated on a BEH HILIC column (50 x 2.1 mm, 1.7 μm; Waters, France) maintained at 30 °C, with positive-mode ionization in a heated electrospray (HESI) source. An Ultimate 3000 UPLC (Thermo Fisher) pumped a binary solvent mixture (solvent A, 5 mM aqueous ammonium formate; solvent B, 0.1 % formic acid in acetonitrile (ACN)) at 500 μL/min using the following gradient: (% B: 0–0.7 min, 95 %; 0.7–1.0 min, 95–5 %; 1.0–2.0 min, 5 %; 2.0–3.0, 5–95 %; 3.0–4.0, 95 %). The following ion transitions were monitored on a TSQ Quantis triple-quadrupole MS/MS: *m/z* 205.1–84.1 and 205.1–130.1 for CML (quantification and confirmation ions, respectively); *m/z* 207.1–84.1 for CML-d_2 internal standard; *m/z* 147.1–84.1 and 147.1–130.1 for lysine (quantification and confirmation ions, respectively); *m/z* 155.2–92.2 for Lysine-d_8 internal standard.

Samples of colon and ileum were analysed using an Accela HPLC system (ThermoFisher) fitted with a Raptor PolarX column maintained at 40 °C (100 x 2.1 mm, 2.7 μm; same-phase guard column 5 x 2.1 mm, 2.7 μm; Restek, France), and the eluent introduced to a TSQ Quantum Ultra MS/MS (ThermoFisher) using HESI+mode. Solvent A (10 % 200 mmol/L ammonium formate in ACN) and Solvent B (0.5 % formic acid) were pumped at 500 μL/min (% B: 0–3.5 min, 12 %; 3.5–8 min, 12–70 %; 8–13 min, 12 %). The following ion transitions were monitored: *m/z* 205.1–130.1 and 205.1–84.1 for CML (quantification and confirmation ions, respectively); *m/z* 207.1–130.1 for CML-d_2 internal standard; *m/z* 147.1–130.1 and 147.1–84.1 for lysine (quantification and confirmation ions, respectively); *m/z* 149.1–131.1 for Lysine-$^{15}N_2$ internal standard.

2.3. Malondialdehyde (MDA), protein carbonyl derivatives (PC), and myeloperoxidase (MPO) assays

The MDA and PC assays were performed in plasma samples using the TBARS Assay kit (Product ref. 10009055) and Protein Carbonyl Assay kit (Product ref. 10005020) provided by Cayman Chemical Company, according to the manufacturer's instructions. Absorbances were measured at wavelengths of 530–540 nm for MDA quantification and at 360–385 nm for PC quantification on a 96-well plate reader (SpectroStar Nano, BMG Labtech). MPO activity was measured in ileum and colon tissue samples as previously described by (ALJahdali et al., 2017).

2.4. RT-qPCR

Tissue samples (kidneys, ileum, colon, and spleen) were preserved in RNA Later and frozen (−80 °C) until analysis. Total RNA extraction was performed with TRIzol™ Reagent (Invitrogen) protocol. Reverse transcription was performed with the High-Capacity cDNA RT Kit (Applied Biosystems) from 1 μg of total RNA. After cDNA synthesis, the relative expression of candidate genes was evaluated by real-time PCR using the PowerUp™ SYBR™ Green Master Mix (Applied Biosystems) on QuantStudio 3 System (Applied Biosystems). Primers were designed according to the following parameters: PCR products with lengths between 80–20 nucleotides; primer dissociation temperature of 58–62 °C with a maximum difference of 2 °C; CG content between 40 and 60 % and oligonucleotide size between 18 and 23 nucleotides. For the analysis of relative expression, cDNA samples were diluted 100x for the quantification of the expression of target genes relative to the endogenous control gene, PPIA, and β-actin. Primer pairs for all gene expression analyses are listed in Table S1. Reactions (10 μL final volume), conducted in three technical replicates, contained 2.5 μL of diluted cDNA, 5 μL of SYBR, 0.5 μL of primers mix (5 mM each), and 2 μL of deionized water. Relative expression was assessed using the ΔΔCt method (Livak & Schmittgen, 2001).

2.5. Metagenomic analysis

Samples of cecal lumen were prepared in an anaerobic environment before undergoing DNA extraction and sequencing (GenoScreen, Lille, France). The V3 and V4 regions of the 16S rRNA gene were amplified using a standardized protocol for amplicon library preparation from GenoScreen and subsequently sequenced on the Illumina MiSeq (Illumina, San Diego,USA), as described elsewhere (Burdet et al., 2019). The data analysis was carried out on Metabiote® v2.0, an alternative pipeline built upon the QIIME workflow (Bolyen et al., 2019), followed by the utilization of DADA2 software for the identification of Amplicon Sequence Variants (ASVs) and taxonomic information. Alpha-diversity in each lumen sample was evaluated using the Chao1 and Shannon diversity indices. A custom workflow was employed for analysing microbial beta diversity, representing operational taxonomic unit (OTU) abundances and multivariable association utilizing phyloseq (McMurdie & Holmes, 2013), microbiome and MaAslin2 packages from BiocManager (Mallick et al., 2021), and fantaxtic package for abundance (Teunisse, 2022) within the R software environment (R 4.3.1). The microbiota data was visualized using multidimensional scaling (MDS) based on the Bray-Curtis similarity index. Significance testing for abundance comparisons was performed using non-parametric Kruskal–Wallis tests followed by Dunn's post-hoc test for pairwise multiple comparisons. Significance was determined at $\alpha = 0.05$. Microbiome Multivariable Association with Linear Models (MaAslin2) was also used to determining associations between microbiome and metadata; multiple tests were controlled using False Discovery Rate (FDR) correction, computed through the Benjamini-Hochberg method.

2.6. Data management and statistical analysis

Data were treated with R version 4.2.1 making use of integrated statistical RStatix, GGPubR, and GGPLOT2 packages (R Core Team, 2022). Data were primarily evaluated for normal distribution fit using the Shapiro-Wilk test. Non-parametric comparisons proceeded including Wilcoxon Test or Kruskal-Wallis rank test followed by Dunn's multiple comparison test when appropriate. All data were presented as means ± Standard Error of Mean (SEM) (bar plots), or median + quartiles (box plots) when considered pertinent. Statistical significance was assessed using $\alpha = 0.05$ as a threshold. Correlations were calculated using Corrplot R package, again using $\alpha = 0.001$ as a threshold. Principal Component Analysis were performed using FactoExtra package.

3. Results and discussion

In this study, the short and long-term effects of a diet rich in dCML were explored in a healthy rodent model. For the first time, to our knowledge, we investigated the physiological outcomes of exposure to a dCML-enriched diet compared with a control diet (STD), during early life (including the breeding period), and up to 70 weeks of age, and in both male and female WT and RAGE KO mice. Despite considerable efforts to ensure an appropriate sample size per group, we acknowledge that the limited number of 6-week-old animals constrained statistical inference. While data for the 6-week-old mice are provided in the supplementary material, they should be interpreted with caution.

3.1. Diet quality, food consumption, and animal physiology at 35 and 70 weeks of age

The two diets employed in this study were closely matched in terms of energy content, ensuring similar calorie, lipid, fibre, and carbohydrate intake across experimental groups (Table 2). Total protein (159.4——162.4 mg/g DW) and lysine (10.9——11.2 mg/g DW) contents were not different between the diets ($p > 0.05$, Table 2). The amount of dCML added to the diets was based on a previous publication by our group (205.6 ± 25.6 μg/g DW) (Grossin et al., 2015). There was a significant, 13-fold difference in dCML contents between the standard (STD) diet (20.8 ± 5.1 μg/g DW) and the diet enriched with dCML (255.2 ± 44.5 μg/g DW) ($p < 0.001$).

Regarding food intake, while RAGE KO mice on the STD diet exhibited significantly lower consumption ($p < 0.01$), all other groups showed similar consumption levels (4.2 ± 0.5 to 5.7 ± 1.1). Despite consuming less food, this behaviour did not affect the overall dCML intake of RAGE KO mice on the STD diet ($p > 0.05$). The glycation of proteins is known to coincide with the formation of colours and aromas that influence dietary choices (Starowicz & Zieliński, 2019). However, the methods we developed and used to synthesise glycated proteins (Nogueira Silva Lima et al., 2023) did not have an effect on food intake *per se*.

At the age of 35 weeks, the median (g) [IQR] weights were estimated to be 32.1 [24.4:42.9] g for females and 40.9 [29.9:46.6] g for males. At 70 weeks of age, the corresponding weights were 42.9 [36.2:49.2] g for females and 46.2 [37.4:56.4] g for males (Table 3). No statistically significant differences in weight measures were evident among the different dietary groups within either age category. The lower food consumption described in the RAGE KO mice on the STD diet did not lead to weight discrepancies compared with the other experimental groups. This suggests that the dCML diet did not have a noticeable impact on overall changes in weight when compared with the STD diet. For both genders, weights fell within the physiological range expected for healthy C57Bl/6 animals at these respective ages (The Jackson Laboratory, 2022). Similar results were observed within 6-week-old animals (Table S2). In addition, RAGE knockout did not appear to disrupt the physiological characteristics of these animals, with both WT and RAGE KO animals exhibiting comparable weights. Neither increased mortality nor obesity was observed to be associated with any of the factors examined in this study (*i.e.* diet, genotype, age).

Table 2
Diet composition, and dCML quantification of the different mouse diets.

Parameter	Units	Diet	
		STD	dCML
Calories	kcal/g	3.1 ± 0.3	3.1 ± 0.3
Fatty acids	%	3.1 ± 0.3	3.1 ± 0.3
Fibers	%	3.9 ± 0.3	3.9 ± 0.3
Carbohydrates	%	46.7 ± 4.6	46.7 ± 4.6
Proteins	mg/g DW	162.4 ± 6.0	159.4 ± 8.8
Lysine	mg/g DW	11.2 ± 1.0	10.9 ± 0.9
Total dCML	μg/g DW	20.8 ± 5.1	255.2 ± 44.5*

DW: dry weight. Total dCML=free and protein-bound CML. * $p < 0.001$. Statistical tests corresponded to comparisons within lines.

3.2. A diet enriched in dCML increases free CML in multiple organs

Free and protein-bound CML were quantified by LC-MS/MS in different organs (kidneys, skin, ileum and colon) of animals in receipt of either a STD or dCML diet (Fig. 2). Animals under a dCML diet showed a significant increase in free CML in the digestive and renal systems, as evident in the kidneys (Fig. 2A), ileum (Fig. 2C), and colon (Fig. 2D), compared with those on a STD diet, regardless of age. Conversely, there was no significant difference between these treatments in free CML concentrations in the skin. In the kidneys, free CML concentrations were significantly different between the two diet groups, being 69.9 ± 19.8 pmol/mg of tissue in the STD group and 197.1 ± 48.2 pmol/mg of tissue in the dCML group ($p < 0.001$) (Fig. 2A). Skin samples showed similar concentrations of free CML between STD and dCML diet groups, measuring 40.8 ± 4.3 and 47.9 ± 8.5 pmol/mg of tissue, respectively (Fig. 2B). The ileum exhibited a 17-fold difference in free CML levels between the STD and dCML diet groups: 4.0 ± 1.9 versus 73.9 ± 29.4 pmol/mg of tissue, respectively ($p < 0.001$) (Fig. 2C). A greater difference (20-fold) was observed in colon samples between the STD (1.2 ± 0.8 pmol/mg of tissue) and dCML diet groups (23.6 ± 17.7 pmol/mg of tissue) ($p < 0.001$) (Fig. 2D). A similar trend was observed in 6-week-old animals (Figure S1). Notably, free CML accumulation occurred in various organs in a diet-dependent manner, and this accumulation was independent of sex or RAGE deletion ($p > 0.05$).

When analysing the levels of protein-bound CML, slight differences were noted, particularly in renal tissue (Fig. 2E), in animals that were exposed to the dCML-enriched diet. Nevertheless, none of these differences were statistically significant. Similarly, no significant differences in dermal protein-bound CML were observed (Fig. 2F). Protein-bound CML concentrations wereunaffected by either sex or RAGE deletion ($p > 0.05$). A similar pattern was observed in 6-week old animals (Figure S1).

Our study thus confirmed an increase in free CML levels resulting from consumption of a dCML-enriched diet compared with a STD diet. This observation aligns with our previous research, and further suggests that the accumulation of exogenous dCML occurs independently of RAGE (Tessier et al., 2016). We have previously shown that a dietary source containing an isotopic, protein-bound ^{13}C-dCML accumulates predominantly in the kidneys, ileum and colon. Our current data confirms that these organs are major sites of accumulation for exogenous dCML. A recent study by van Dongen et al. (2021) demonstrated elevated free CML levels in the kidneys, liver, and plasma of mice fed with a baked chow diet high in dCML (40 μg dCML/g). Other workers have also reported a higher accumulation of dCML in organs of the digestive-excretory system, which serves as the primary interface for environmental toxicants, including dietary neoformed compounds (Sarron et al., 2020).

To the best of our knowledge, this study represents the first exploration of the impact of prolonged consumption of a dCML-enriched diet

Table 3
Weight (g) distribution among female- and male mice of 35 and 70-week-old. Values represent median (g) [IQR].

Age (Weeks)	Diet	Females				Males			
		WT		RAGE KO		WT		RAGE KO	
		n	Weight(g) Median [min:max]	n	Weight(g) Median [min:max]	n	Weight(g) Median [min:max]	n	Weight(g) Median [min:max]
35	STD	8	30.3[24.6:37.2]	11	31.0[24.4:38.1]	12	38.2[29.9:46.5]	7	42.0[39.5:44.1]
	Switch	10	32.3[27.5:42.0]	–	–	3	45.8[45.7:45.9]	–	–
	dCML	10	34.2[24.5:42.9]	5	32.1[28.4:33.7]	3	40.9[31.7:42.7]	7	40.8[37.3:42.7]
70	STD	8	38.5[36.2:42.0]	12	43.7[40.6:47.5]	14	46.8[41.0:56.4]	6	44.0[37.3:51.3]
	Switch	7	44.4[41.6:48.0]	–	–	7	45.2[41.5:51.7]	–	–
	dCML	9	40.4[37.0:49.2]	12	44.2[40.8:46.5]	8	47.4[41.9:53.1]	9	45.8[41.8:49.1]

on CML levels in the skin of an animal model. There is a long-established and widely accepted understanding that AGEs accumulate in a linear fashion over time in human skin collagen (Dunn et al., 1991). On the other hand, dCML accumulation in the skin of a murine model has been reported to be only moderately increased, in a non-linear fashion, with age (Gorisse et al., 2016). In the present study, our observations suggest that neither the diet nor the putative age-related, low-grade disturbances investigated herein led to discernible alterations in either free or protein-bound CML levels in the skin of either strain of mice (Fig. 2B & 2F). We demonstrated by a reliable quantitative method (LC-MS/MS) that neither free nor protein-bound CML accumulated in the skin over 35 or 70 weeks, regardless of dietary exposure to dCML and the putative indirect stresses (*e.g.* dicarbonyl stress, oxidative stress) caused by a high-AGE consumption. However, this finding does not exclude the potential accumulation of dAGEs other than dCML, not explored here.

In the present study, a slight but statistically non-significant rise in protein-bound CML levels was noted in the kidneys of both WT and RAGE KO animals that were administered a dCML diet (Fig. 2E). The lack of effect is in accordance with a recently published study from our research group (Helou et al., 2022), demonstrating that the administration of exogenous dCML in rats did not result in a significant increase in protein-bound CML concentrations in plasma. The lack of significant effects on the formation of protein-bound CML from a diet rich in dAGEs has been consistently reported in various human studies (Linkens et al., 2022; Scheijen et al., 2018). Linkens and colleagues reported no discernible difference in protein-bound CML in plasma before and after a 4-week dietary intervention study that included 82 obese subjects aged between 51–53 years (Linkens et al., 2022). On the other hand, studies investigating the effects of a dCML-enriched diet or baked rodent-chow diet on the kidneys of mice (Teissier et al., 2019; van Dongen et al., 2021) suggest a plausible link between increased protein-bound CML levels and kidney malfunction (*i.e.* glomerular sclerosis) of animals consuming a dCML-enriched diet. Although the protein-bound form of CML predominates in foods (van Dongen et al., 2021), the absorption of dCML by the intestinal epithelium occurs primarily through digested free or dipeptide forms (Hellwig et al., 2011). Therefore, the pool of protein-bound CML in organs or circulation cannot be attributed to a dietary source. Although unexpected, it is nevertheless reasonable to hypothesise that any observed increase in protein-bound CML, as suggested in some previous animal studies (Grossin et al., 2015; van Dongen et al., 2021), stems from the indirect effects of dCML ingestion and accumulation, potentially mediating the activation of glycoxidative stress (Boesten et al., 2014).

3.3. Diet-switching reverses levels of dCML in kidneys, ileum, and colon

The accumulation of free CML was reversed by switching from a dCML diet to a STD-diet at an early stage of life (6 weeks). This diet-switching intervention led to significantly lower free dCML levels in the kidneys, ileum, and colon of animals at both 35 and 70 weeks of age (Fig. 2A, 2C & 2D). Importantly, free CML levels in the switched group were comparable to the "baseline" levels observed in animals that had been continuously fed the STD diet ($p > 0.05$). Our study represents the first demonstration of the reversibility of the effects of high dCML consumption, including the exposure of the parental line to STD and dCML diets during the breeding period. Taking into consideration the differences in free CML content in the kidneys, ileum, and colon, an early-life diet switch returned dCML levels to concentrations similar to those in the control groups. While there is no consensus regarding the specific cellular compartment in which dCML may accumulate, it is logical to assume that exogenous glycation adducts might be primarily associated with the extracellular matrix. These findings are a positive indicator of the potential reversibility of the supposed deleterious effects of dAGEs for human health. To our knowledge, only one other study has explored the potential reversibility of dAGE accumulation, but it did not specifically examine perinatal exposure. Working exclusively on 9-week-old C57BL/6/OlaHsd female mice, van Dongen and colleagues compared some short-term effects of a baked- versus a standard-chow diet, and demonstrated the reversibility of the accumulation of dCML in plasma, liver, and kidneys (van Dongen et al., 2021). In humans, the reversibility of dCML accumulation was previously reported in newborns taking either industrialized infant formulas (high in dCML) or breast milk (low in dCML). This study showed that the difference in plasma dCML concentrations observed in the two infant groups in the first months of life gradually disappeared with subsequent dietary diversification (Šebeková et al., 2008).

3.4. A diet enriched in dCML does not induce notable oxidative stress

A panel of tests was adopted in order to characterise an oxidative stress phenotype encompassing the assessment of systemic MDA levels, plasmatic PC, and MPO activity in ileal and colonic tissues. There were no significant differences in MDA or PC concentrations (Fig. 3A and 3B), nor MPO activity (data not shown), in relation to the different diets, age, sex or genotype of the animals ($p > 0.05$). Subsequently, we assessed the relative expression renal levels of *SOD1*, *SOD2*, and *GLO1* once this organ had been confirmed to accumulate the greatest amount of dCML. No differences in *SOD1* and *SOD2* were observed between the different diets, nor associated with age, sex or genotype ($p > 0.05$) (Fig. 3C and 3D). We then investigated whether a dCML-enriched diet had any impact on *GLO1* mRNA expression (Fig. 3E). While no notable changes in *GLO1* expression were observed in relation to the diet, age or sex ($p > 0.05$), a significant 2-fold increase was noted when comparing RAGE KO with WT animals (Fig. 3E). Animals in the 6-week-old group displayed a similar expression pattern regarding the proposed characterization panel for oxidative stress (Figure S2).

The relationship among MDA, PC, and glycation is intricately tied to oxidative stress, and the interplay between these processes underscores their potential collective importance in oxidative stress-induced molecular damage. Glycoxidative stress, for instance, may occur through various mechanisms such as the autoxidation of glucose, the breakdown of Maillard reaction intermediates, or the interaction between AGEs and RAGE (Rabbani & Thornalley, 2012). Through the simultaneous evaluation of lipid peroxidation, protein carbonylation, and the expression of the genes coding various enzymes, our research has yielded multiple lines of evidence suggesting that the exposure to dCML did not induce

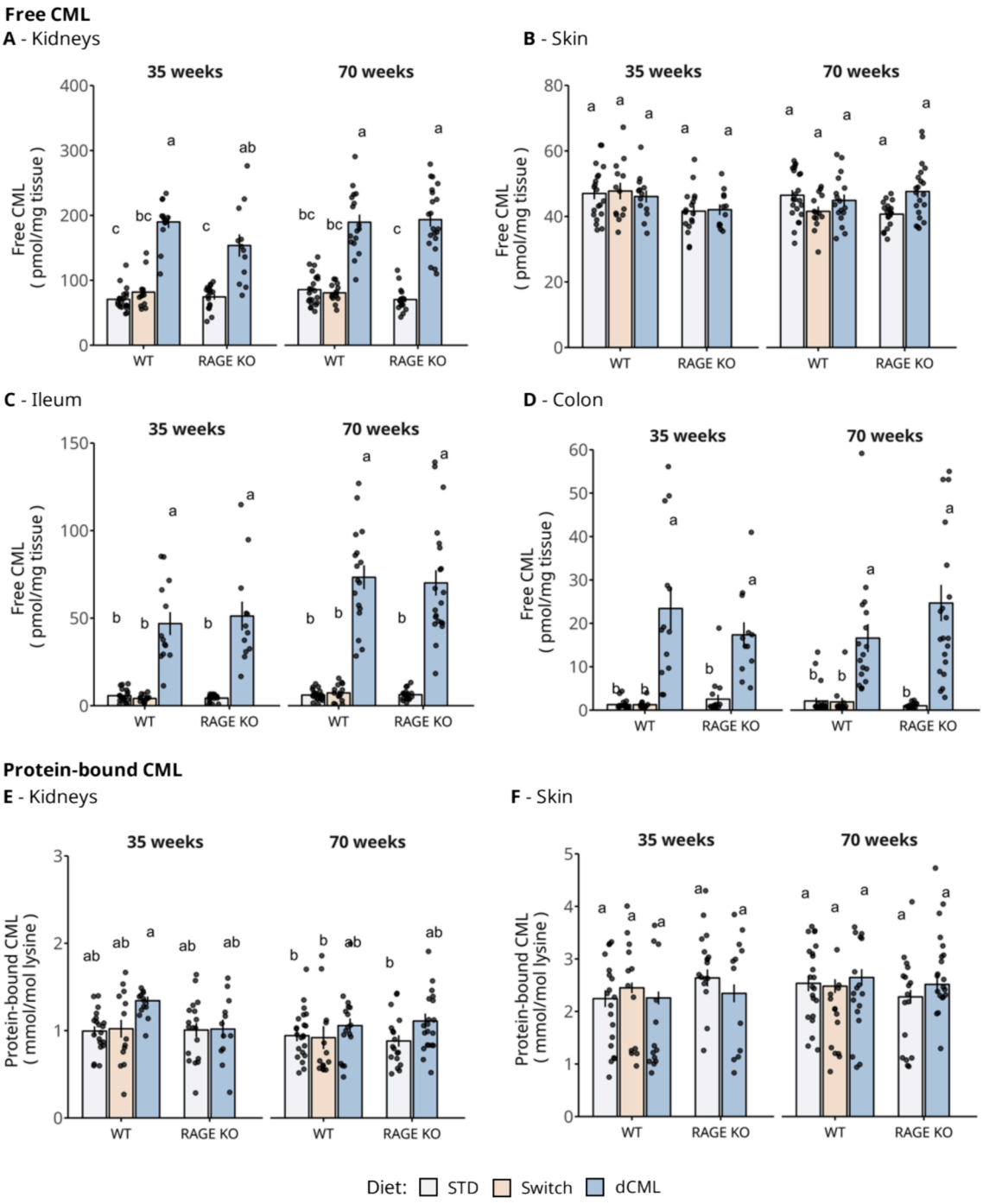

Fig. 2. Free CML quantification by LC-MS/MS in **(A)** kidneys, **(B)** skin, **(C)** ileum, and **(D)** colon, and protein-bound CML quantification in **(E)** kidneys, and **(F)** skin of 35- and 70-week-old C57BL/6 mice (WT and RAGE KO) administered a control (STD), or a dCML-enriched diet (dCML), or which underwent a diet switch from dCML to STD diet at 6 weeks of age. Bars represent means ± SEM. Letter indices (Kruskal-Wallis rank test followed by Dunn's posthoc test for multi-comparisons) indicate statistical differences among groups within each organ. $\alpha = 0.05$. Complementary data on 6-week animals in supplemental Figure S1.

elevated oxidative stress in healthy animals.

Overall, no differences were observed concerning renal cytoplasmic (*SOD1*) or mitochondrial matrix (*SOD2*) superoxide dismutases, suggesting no direct dysfunction in mitochondrial functionality between 35 and 70 weeks of age in mice. It is well-accepted that decline in mitochondrial function is associated with age, and hence with an age-related increase in oxidative stress (Chistiakov et al., 2014). Based on our findings, renal *SOD1* and *SOD2* appeared to exhibit consistent expression levels throughout the entire 70-week lifespan of our animals. On the other hand, the expression of these enzymes in peripheral tissues such as the cardiac arteriolar system has been reported to respond to various stimuli (*e.g.* aging, a high-fat diet). Grossin and colleagues demonstrated the accumulation of dCML in the cardiac arterial tissue and linked it to the subsequent local loss of tissue flexibility. After administering a high-fat diet, Yu et al. (2017) identified an elevation in dCML levels in the same tissue, accompanied by a concurrent increase in MDA and protein carbonylation. This was followed by a decrease in *SOD2* expression, suggesting an escalation of local oxidative stress (Yu et al., 2017). The knockout of RAGE has been suggested to contribute to an upregulation of *SOD2* mRNA expression compared with +/- 90-week-old WT mice

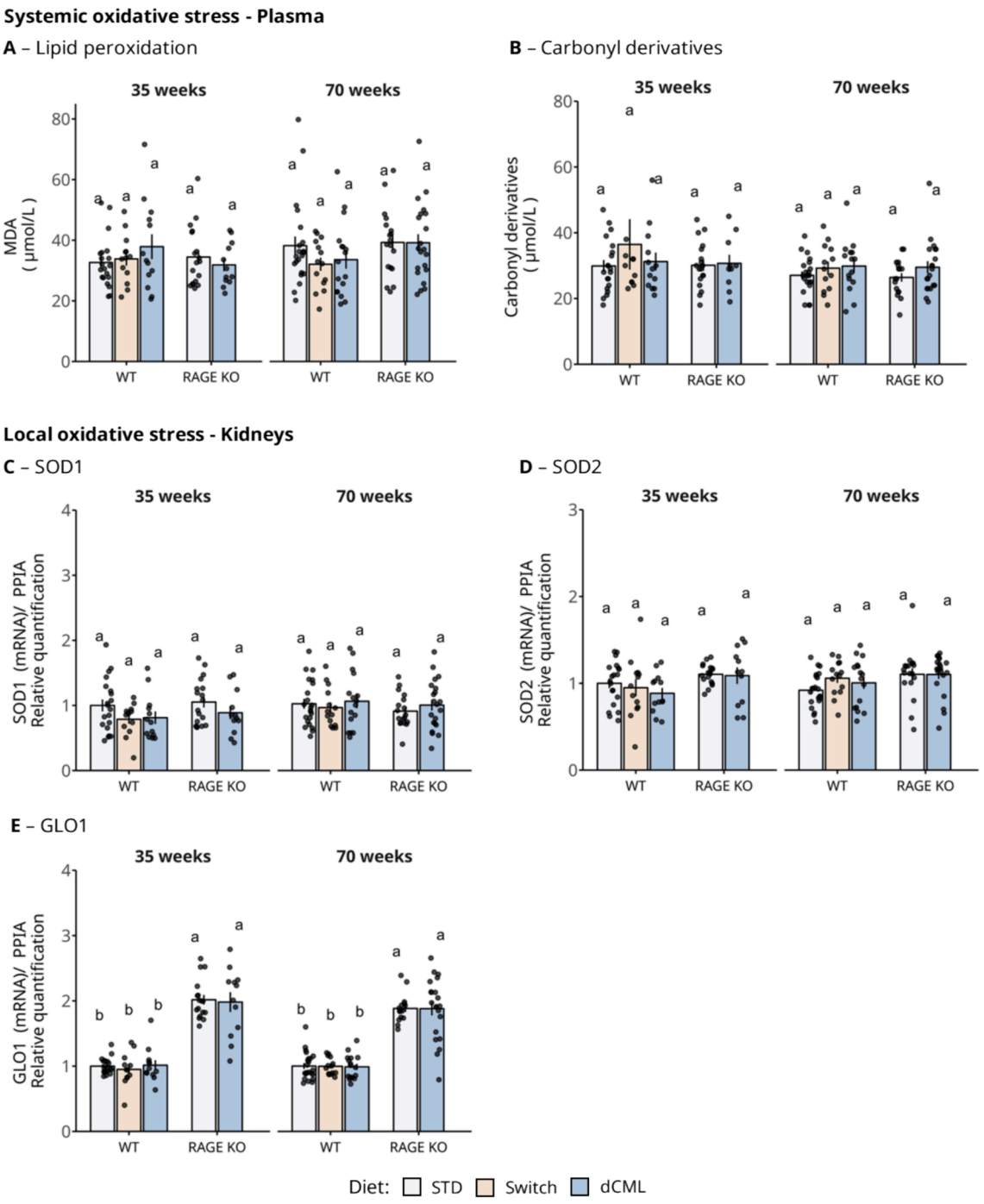

Fig. 3. Oxidative stress assessment in systemic (plasma) and local (kidney) levels across the different dietary treatments in WT and RAGE KO mice between 35 and 70 weeks. **(A)** Lipid peroxidation assessment measured by MDA concentrations (µmol/L); **(B)** Protein oxidation assessment measured by PC derivatives concentrations (µmol/L). Relative expression of **(C)** *SOD1*, **(D)** *SOD2* and **(E)** *GLO1* from RT-qPCR on kidney samples. Bars represent means ± SEM. Letter indices (Kruskal-Wallis rank test followed by Dunn's posthoc test for multi-comparisons) indicate statistical differences among groups within each chart. $\alpha = 0.05$. Housekeeping gene: PPIA. Reference group: WT-STD-35-week animals. Complementary data on 6-week animals in supplemental Figure S2.

(Teissier et al., 2019). Although not statistically significant ($p > 0.05$), a comparison of our results in mice at 35 and 70-week-old (Fig. 3D) would seem to reflect the trend described by Teissier and colleagues (2019).

A *GLO1* gene duplication emerged as an artifact from multiple backcrossing in the RAGE KO lineage (Bartling et al., 2020). Widely considered a "vitagene", *GLO1* is linked to decreased oxidative stress and increased lifespan and exhibited a 2-fold increased expression in RAGE KO mice compared with WT animals. While acknowledging this genetic artifact, our focus on *GLO1* aimed to unveil potential anti-glycation mechanisms countering dAGEs' deleterious effects. Despite the elevated *GLO1* expression, no significant reduction in oxidative stress biomarker expression was observed in RAGE KO mice at either systemic or local levels (Fig. 3). At the same time, no decrease in protein-bound CML concentration in kidneys or skin was observed over time in RAGE KO mice compared with WT animals (Fig. 2E & 2F). RAGE activation has been suggested to downregulate *GLO1*, leading to heightened endogenous methylglyoxal and methylglyoxal-derived AGEs (Thornalley, 2008). Although comparing protein-bound carboxyethyl-

lysine (CEL) and methylglyoxal-derived hydroimidazolone (MG-H1) formation in WT and RAGE KO mice would have been insightful, it's crucial to note that the increased *GLO1* expression in RAGE KO animals could potentially confound our comparison of genotypes.

3.5. Switching diets during early life appears to affect the development of intestinal sensitivity to inflammation

To further investigate the potential pro-inflammatory effects of a diet enriched with dCML, we conducted additional assessments of RAGE expression, and downstream cascades associated with RAGE activation. Our analysis included measuring mRNA expression levels of the cytokines *TNFα* and *IL6,* which play crucial roles in tissue inflammation.

Across the various organs examined in this study, there were no significant fluctuations in relative RAGE expression with diet, age or sex (Fig. 4A, 4B, 4C). There is broad consensus that the adverse impacts of dAGEs are partly facilitated via the AGE-RAGE axis, which, in turn, is linked to a positive feedback loop involving NFκB-RAGE expression (Lin et al., 2016). Grossin et al., (2009) illustrated that cultured umbilical endothelial cells exhibited a two-fold increase in *RAGE* expression upon prolonged exposure to dCML. *In vivo* studies have demonstrated that diets enriched with methylglyoxal derivatives increased RAGE expression in the brains of C57BL/6 mice (Cai et al., 2014). Nevertheless, our investigation indicates that the levels of RAGE did not change with the *in vivo* accumulation of dietary free CML. We hypothesise that this could be linked to the suggested lower affinity of free CML for RAGE compared with protein-bound CML (Xue et al., 2011), potentially diminishing the adverse impacts that dCML could play in RAGE activation or expression. The absence in the current study of increased levels of protein-bound CML among dCML animals accords well with our observations on the lack of stimulation in RAGE expression in these animals (section 3.2.). A previous study demonstrated a similar pattern of RAGE expression in the

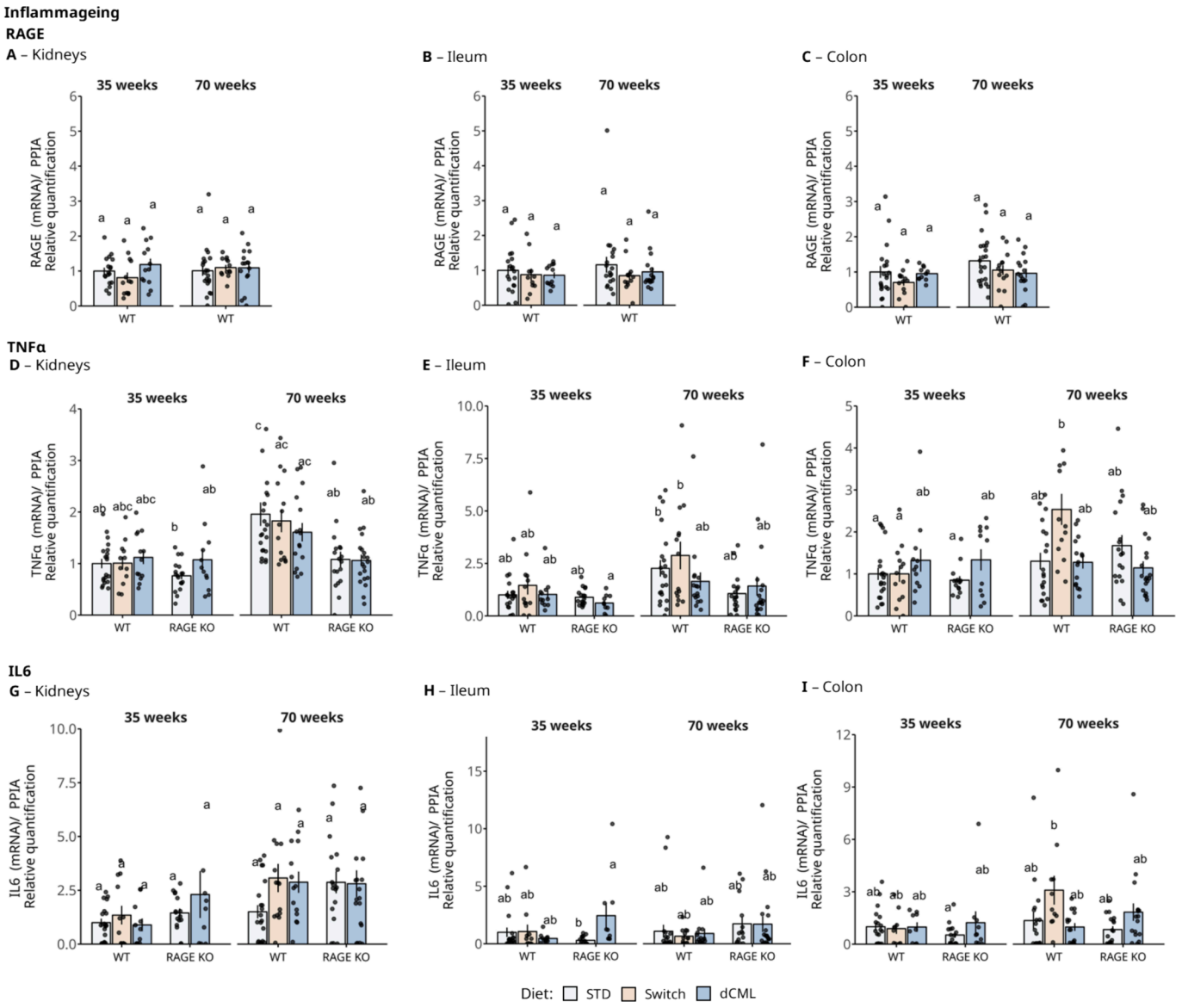

Fig. 4. Inflammageing assessment across the different dietary treatments in WT and RAGE KO mice between 35 and 70 weeks. Relative expression of *RAGE* across the different dietary treatments administered to WT and RAGE KO mice for 35 and 70 weeks in **(A)** kidneys, **(B)** ileum, and **(C)** colon. Relative expression of *TNFα* across the different dietary treatments administered to WT and RAGE KO mice for 35 and 70 weeks in **(D)** kidneys, **(E)** ileum, and **(F)** colon. Relative expression of *IL6* across the different dietary treatments administered to WT and RAGE KO mice for 35 and 70 weeks in **(G)** kidneys, **(H)** ileum, and **(I)** colon. Bars represent means ± SEM. Letter indices (Kruskal-Wallis rank test followed by Dunn's posthoc test for multi-comparisons) indicate statistical differences among groups within each organ. $\alpha = 0.05$. Housekeeping gene: PPIA. Reference group: WT-STD group 35 weeks. Complementary data on 6-week animals in supplemental Figure S3.

endothelium of the aorta of 48-week-old mice, with no significant transcriptional changes being attributable to diet at a comparable dose of 200 μg dCML/g food (Grossin et al., 2015). However, differences only became apparent through statistical analysis of immunohistochemical data in the study by Grossin and colleagues, indicating a 2-fold increase in RAGE protein expression in the aortic tissue.

Diet, age and genotype all had small but discernible impacts upon expression of inflammatory biomarkers *TNFα* and *IL6*, in particular in the Switch group, and most evident in the colon samples (Fig. 4F and 4I). It is widely recognized that introducing complementary feeding too early in life can influence intestinal homeostasis in mammals (Differding et al., 2020; Ribeiro et al., 2024). Early dietary changes have been suggested to reduce integrity of the intestinal epithelium, altering microbial diversity and inducing fluctuations in the levels of short-chain fatty acids (Differding et al., 2020). Such alterations are closely linked to intestinal sensitivity and the onset of inflammatory responses (Caminero et al., 2019; Gill et al., 2022; Plunkett & Nagler, 2017). Given the association of glycation and protein allergenicity (Toda et al., 2023), our interpretation of these data centres on the idea that, compared with the other groups, animals in the Switch group may have been rendered more susceptible to intestinal inflammation as a result of dietary changes early in life.

The inflammatory effects of dAGEs continue to arouse debate, with recent research presenting conflicting conclusions in animal models. Historically, AGEs have been associated with pro-oxidative processes compromising the vasculature in rodent and rabbit animal models. Studies have suggested the involvement of consuming glycated BSA, or a glycation precursor (*e.g.* methylglyoxal), in complications associated with diabetes and atherosclerosis (Illien-Jünger et al., 2015; Vlassara et al., 1992). More recently, investigations over 22 weeks in male, C57BL/6 mice fed a diet rich in AGEs (containing casein-methylglyoxal at 17.4 $g_{MG\text{-}H1}/kg_{food}$) revealed greater levels of pro-inflammatory cytokines including Il1β, IL17, and TNFα. This was accompanied by a suppression of anti-inflammatory mediators such as IL10 and IL6 (Mastrocola et al., 2020). Despite using a different experimental procedure, our findings closely resemble those of a recent study carried out by van Dongen et al. (2021) wherein heated animal feed was provided over a 10-week period. Van Dongen and colleagues revealed that a baked chow diet had only a marginal pro-inflammatory impact in plasma samples from C57BL/6 female mice (van Dongen et al., 2021). The authors evaluated six inflammation biomarkers, including CRP, TNFα, INF, KC/GRO, IL6, and IL10. Notably, only the systemic levels of the anti-inflammatory cytokine IL10 displayed a significant decrease when mice were fed a baked-chow diet, while inflammatory biomarkers remained unaffected by diet (van Dongen et al., 2021). These recent discoveries parallel our own observations, indicating that the proinflammatory effects of short- or long-term dietary exposure to AGEs appear to be limited, at least within the healthy mouse models used in both studies. Similar to the progression of research using animal models in the field of glycation, humans consuming diets rich in AGEs have been specifically associated with microvascular complications in diabetic patients and cognitive decline due to the glycoxidative effect of these so-called "glycotoxins" (Beeri et al., 2011; Negrean et al., 2007). In humans, considering the most recent and robust evidence, there have been no reported correlations between concentrations of dAGEs and inflammation, oxidative stress, or changes in insulin metabolism, even in obese individuals with comorbidities (Linkens et al., 2022).

Significant age-related changes in *TNFα* (Fig. 4D, 4E, 4F) and *IL6* expression (Fig. 4G, 4H, 4I) were primarily noted in the kidneys. Different *TNFα* expression was observed between 70-week-old WT mice and age-matched RAGE KO mice, suggesting a potential protective role of RAGE knockout in mitigating pro-inflammatory expression within the kidneys ($p < 0.001$). Earlier findings from our research group described comparable trends by comparing renal tissues from 20-month-old WT and RAGE KO animals, contrasted with those of their 3-month-old counterparts (Teissier et al., 2019). In older mice, an upregulation of *TNFα* and *VCAM1* compared with younger animals had already been observed by others in various fluids and tissues, including plasma and brain (Ishikawa et al., 2016; Miró et al., 2017; Yousef et al., 2019). Teissier et al. (2019) took into consideration that, besides the putative involvement of dCML in the aggravation of nephropathies, age was a preponderant factor in the variation of *TNFα* and *VCAM1*. This age-related factor could be a confounding variable when distinguishing the actual effects of the diet in our study context. In addition, in this same study, RAGE deletion was reported to be associated with reduced inflammation (Teissier et al., 2019).

3.6. Increased consumption of dCML does not result in accelerated cellular senescence in healthy animals

Levels of critical senescence regulators were assessed within renal and splenic tissues in order to investigate the influence of a high-dCML diet on cellular immune senescence. Our analysis revealed no accelerated senescence attributable to diet, genotype, or sex on the relative expressions of *SIRT1*, *P16*, and *GLβ1* mRNA, as illustrated in Fig. 5. Similar patterns were noted in the gene panels of either kidneys or spleen, with the exception of a significant age-related alteration in *P16* ($p < 0.001$) expression in the spleen of both genotypes, indicating the impact of age on immune senescence. Similar fold-changes were observed in animals of 6-weeks compared to 70-week-old animals (supplementary Figure S5).

Although nutrition is one of many factors that can contribute to the worsening of age-related dysfunctions, including cellular senescence (*e.g.* mTOR responsiveness to caloric restriction), our findings suggest that dCML intake does not appear to impact cellular senescence. It is thought that SIRT1 functions by deacetylating proteins within the nucleus, encompassing histone proteins and non-histone targets such as AKT/mTOR and FOXO (Alves-Fernandes & Jasiulionis, 2019). However, feeding mice a diet abundant in glycation products (mainly dCML) was suggested to diminish *SIRT1* activity in aortic walls (Grossin et al., 2015). This reduction was inferred to be potentially associated with arterial aging, as indicated by decreased flexibility of this tissue being concomitant with increased dCML accumulation (Grossin et al., 2015). Suppression of *SIRT1* linked to AGE consumption has also been associated with muscle oxidative stress and insulin resistance (Cai et al., 2012). Despite implementing a comparable experimental design to that of Grossin and colleagues (2015), we did not observe the same effects in the kidneys or in the spleen, suggesting a null effect beyond the endothelial level (Fig. 5A, 5B). Nevertheless, the precise connections between RAGE and SIRT1 remain incompletely understood, and RAGE KO mice have been suggested to exhibit diminished ageing-related indicators and *SIRT1* activity (Teissier et al., 2019). Our study found no similar effect on *SIRT1* expression in either kidney or spleen, possibly due to the cells' phenotypic plasticity to the accumulation of free CML.

Increased expression of *P16* (Fig. 5C, 5D) has been reported to correlate with the progression of senescence. When combined with *GLβ1* (Fig. 5E, 5F), *P16* comprises a senescent phenotype which primarily serves to activate downstream survival pathways (Hall et al., 2017). There is a growing interest on understanding the role of T cells in ageing due to their influence on overall immune responses (Mittelbrunn & Kroemer, 2021). The age-related increase in *P16*, documented extensively in the literature, is recognized as a hallmark of T cell aging and a consequent decline in the immune system remains a significant health concern (Lee et al., 2022). Senescent T cells exhibit additional markers of ageing. However, despite these changes, we observed no simultaneous increase in *GLβ1* levels, or even in various other cellular actors associated with T cell differentiation such as *FOXP3, GATA3, RORγt,* and *T-BOX21* (Figure S6). This suggests that in our study, neither premature nor uncontrolled senescence phenotypes were induced by either dietary factors or ageing.

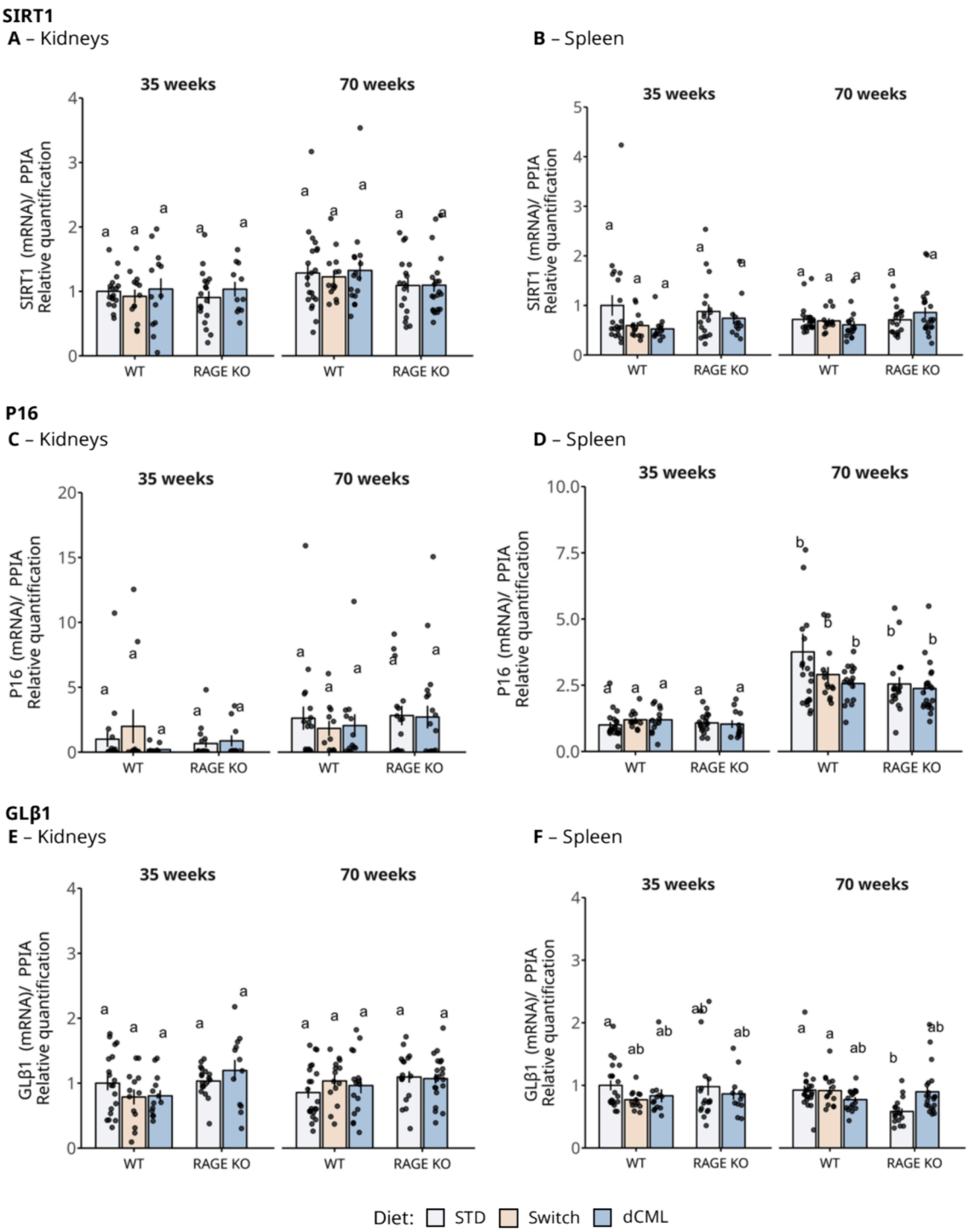

Fig. 5. Senescence assessment across the different dietary treatments in WT and RAGE KO mice between 35 and 70 weeks. Relative expression of *SIRT1*, *P16*, and *GLβ1* from RT-qPCR analysis. Relative expression of *SIRT1* across the different dietary treatments administered to WT and RAGE KO mice at 35 and 70 weeks in **(A)** kidneys and **(B)** spleen. Relative expression of *P16* the different dietary treatments administered to WT and RAGE KO mice at 35 and 70 weeks in **(C)** kidneys and **(D)** spleen. Relative expression of *GLβ1* the different dietary treatments administered to WT and RAGE KO mice at 35 and 70 weeks in **(E)** kidneys and **(F)** spleen. Bars represent means ± SEM. Letter indices (Kruskal-Wallis rank test followed by Dunn's post hoc test for multi-comparisons) indicate statistical differences among groups within each chart. α = 0.05. Housekeeping gene: PPIA. Reference group: WT-STD group 35 weeks. Complementary data on 6-week animals in supplemental Figure S5.

3.7. Biomarkers of low-grade stress are correlated in aged mice

Although the prolonged intake of a dCML-enriched diet did not provoke notable impacts upon WT or RAGE KO mice, a comprehensive correlation analysis was performed to highlight the potential relationships among low-grade stress indicators. Fig. 6 illustrates correlation plots combining dCML measurements with gene expression patterns associated with renal inflammation, oxidative stress and immunosenescence. By focusing solely on correlations with a threshold of α = 0.001, we identified strong associations in the kidneys (Fig. 6A), ileum (Fig. S7A), and spleen (Fig. S7B), but no notable associations in skin, colon, or plasma (data not shown). Overall, the correlations revealed

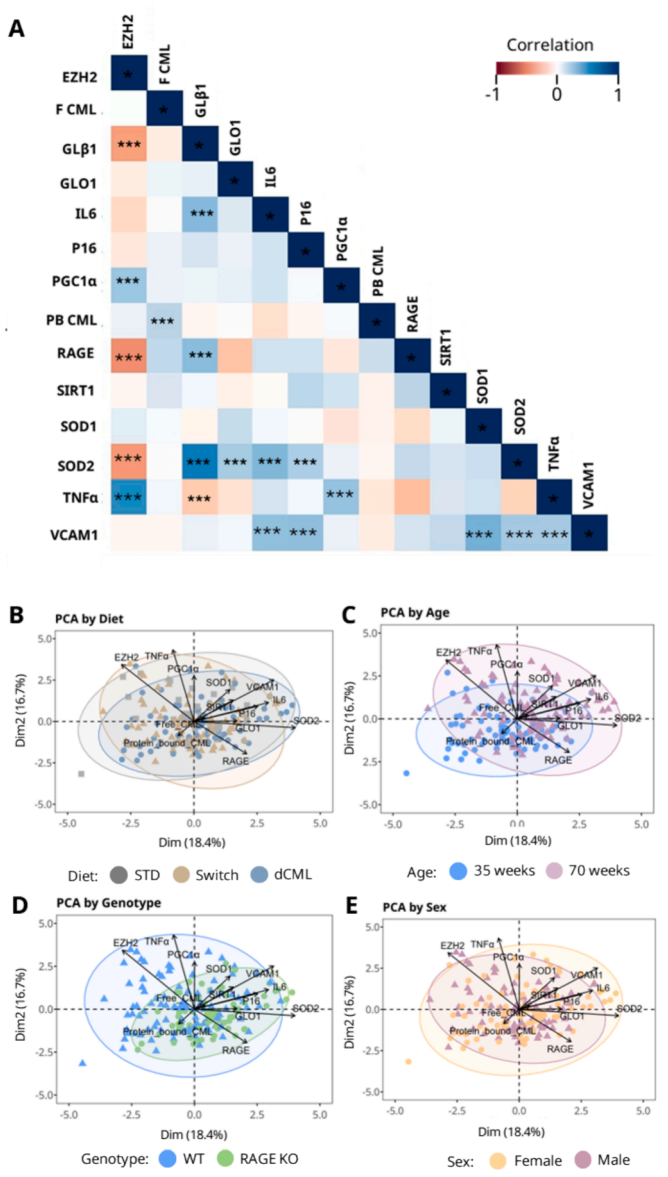

Fig. 6. Analysis of **(A)** correlation and PCA between multiple biomarkers related to glycation, oxidative stress, inflammation, and senescence in the kidneys sorted by **(B)** diet, **(C)** age, **(D)** genotype, and **(E)** sex. *** $p < 0.001$.

that fluctuations in levels of free or protein-bound CML in kidney and ileum were not strongly linked to changes in biomarker levels. Considering the more comprehensive panel of biomarkers analysed in the renal tissue, a strong correlation was noted among a cluster of biomarkers related to oxidative stress (*SOD1, SOD2*), senescence (*EZH2, GLβ1, PGC1α*), and inflammation (*IL-6, TNFα, VCAM-1*), as depicted in Fig. 6A (Individual data on *EZH2* and *PGC1α* are presented in Figure S4 A/B). In the ileum (Fig. S7A), only one negative correlation was evident, between *TNFα* and *RAGE*. In the spleen (Fig. S7B), positive correlations were revealed among the majority of screened genes. Although not all proposed genes in the splenic panel show direct connections, many are linked through similar regulatory pathways or participation in T-cell differentiation.

Although a causal relationship cannot be established from these results, it seems safe to say that there exists a synergistic effect among the measured biomarkers, as evidenced by a subtle yet significant evolution in the expression of multiple markers, particularly in the kidneys. These correlations, supported by the PCA analysis, underscore that diet had no effect on biomarkers between groups (Fig. 6B). The primary drivers of these differences appear to be inflammation mediators such as *TNFα* and RAGE deletion (Fig. 6C and 6D). As previously described, *TNFα* expression correlated with age increase, and 70-week-old RAGE KO mice consistently exhibited lower expression compared with age-matched WT mice (Fig. 4D). Age is suggested to have a role in driving the progression of biomarker expression in this experimental context (Fig. 6C). These correlations accord with the widely acknowledged phenomena attributed to inflammageing, and partly corroborate the proposed protective effect of RAGE deletion (Fig. 6D) (Ferrucci & Fabbri, 2018; Teissier et al., 2022). Consistently across our results, it appears that sex is not a factor in the physiological responses investigated here (Fig. 6E).

Further, our results indicate that the relationships between RAGE and the stress biomarkers examined do not support the notion of a positive feedback loop, as previously proposed in the literature (Bongarzone et al., 2017). Our hypothesis suggests that elevated RAGE expression at the genetic level may not be necessary for the onset of low-grade stress. The genesis of such a mechanism might be related to the multiple cellular receptors (*e.g.* Toll-like receptors, TLRs) with overlapping functions which also participate in pro-inflammatory responses (Kawai & Akira, 2010). It is important to recognize that cellular receptors can be redundant in activating specific molecules, potentially obscuring the nuanced effects of receptors like RAGE. Hence, TLR4 is a critical component of the innate immune system, primarily serving as a pattern recognition receptor (Zhong et al., 2020). Upon activation, TLR4 initiates signalling cascades that lead to the production of a range of inflammatory mediators and regulators, as well as the expression of genes correlated to immune responses such as *TNF-α*, *IL-6*, *SOD2* (Gao et al., 2021; Moretti et al., 2023; Setiawan et al., 2022; Zeuke et al., 2002). Despite these considerations, while there were no notable increases in RAGE mRNA expression, its deletion appears to inhibit the inflammation trigger, although the underlying mechanism remain to be clarified.

3.8. *The gut microbiota is minimally influenced by diet and age*

Metagenomic analysis was employed to assess bacterial diversity and abundance in animals aged 35 and 70 weeks, with a focus on conserved regions of the 16S gene. Although α-diversity richness (Chao1, Figure S8A) and evenness indices (Shannon, Figure S8C) fluctuated with age, no statistical significance was observed. These findings suggested that microbial communities within the samples were resilient, with no dominant taxon significantly emerging from influences of diet, age, or genotype. Similarly, the Bray-Curtis dissimilarity test, used to evaluate β-diversity, revealed a minor time-dependent evolution (Figure S9). Comparing animal groups at 35 and 70 weeks of age, we observed that microbial communities became more uniform in older animals. However, at neither age was a clear diet-dependent clustering evident.

In general terms taxon abundance corresponded to what has long been known, with a predominance of Firmicutes and Bacteroidota taxa (Magne et al., 2020). The global abundance of microbiota was assessed at 35 and 70 weeks, revealing Firmicutes as the dominant phylum, comprising nearly 61 % of bacterial relative abundance across all genotypes and diets (data not shown). Within Firmicutes, the Lachnospiraceae families were particularly prevalent. Bacteroidota accounted for approximately 23 % of relative abundance, with notable representation from Alistipes and Muribaculaceae. Surprisingly, minor phyla like Desulfobacterota (predominantly Desulfovibrio) and Verrucomicrobiota (mainly Akkermansia) exhibited relatively high abundance, ranging from 7.6 % to 11.3 % and 1.5 % to 5.8 %, respectively. Although these taxa showed, on average, higher abundance within aged mice compared to prior studies (Ratto et al., 2022), no significant differences were observed among groups in our dataset. Furthermore, the equilibrium between the main phyla, Firmicutes and Bacteroidota, was supported by their consistent ratio of around 2.7 across different timepoints, diets, and genotypes (Fig. 7B). The Firmicutes/Bacteroidota (F/B) ratio is

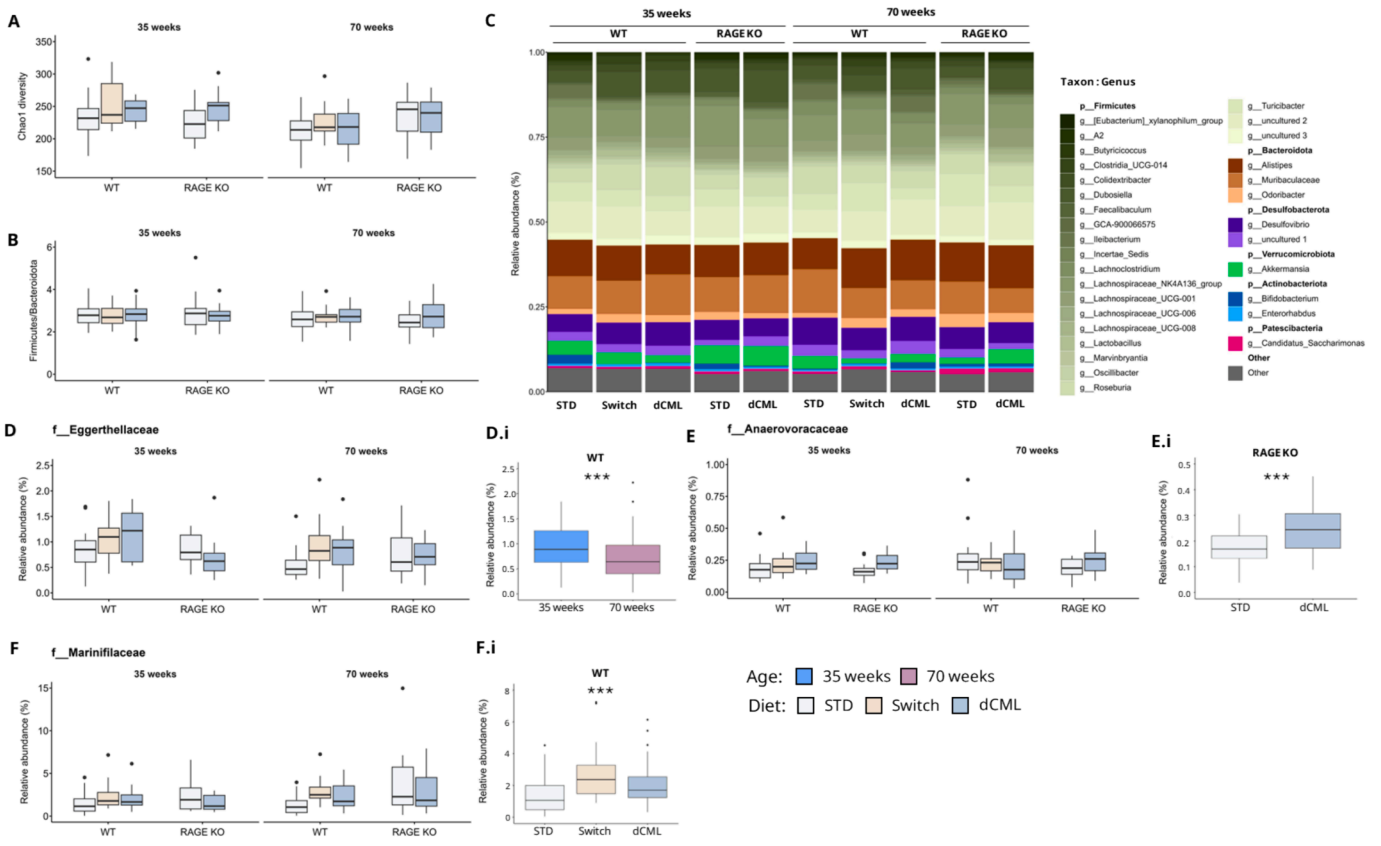

Fig. 7. Cecal microbiota analysis of 35 and 70-week-old WT and RAGE KO mice submitted to a STD or dCML-diet. **(A)** Chao1 α-diversity; **(B)** Firmicutes/Bacteroidota ratio; (C) Genera relative abundance; **(D)** Eggerthellaceae family relative abundance; **(D.i)** Eggerthellaceae relative abundance regrouped by age within WT animals; **(E)** Anaerovoracaceae family relative abundance; **(E.i)** Anaerovoracaceae relative abundance regrouped by diet within RAGE KO animals; **(F)** Marinifilaceae family relative abundance; **(F.i)** Marinifilaceae relative abundance regrouped by diet within RAGE KO animals. *** $p < 0.001$. Statistical multivariate significance. Corresponding data on 6-week-old animals are presented in Figure S8.

known to be influenced by different dietary and pathophysiological circumstances (Magne et al., 2020). Research has revealed that a diet rich in MG-H1-casein reduced the F/B ratio in stool samples from 26-week-old male mice submitted to a modified diet for 22 weeks (Mastrocola et al., 2020). A major difference between our study and others exploring the effects of glycation upon intestinal microbial diversity (including Mastrocola et al. (2020)) is our focus on metagenomic analysis of cecal lumen rather than faecal pellets. This may complicate comparisons of our data with other studies (Tanca et al., 2017).

Although the overall changes in abundance were not significant (Fig. 7C), a detailed analysis to detect subtle variations in taxon distribution was conducted. Using a multivariate workflow (MAasLin2), statistically significant differences linked to age and diet within minor microbial communities such as Eggerthellaceae (Fig. 7D), Anaerovoracaceae (Fig. 7E), and Marinifilaceae (Fig. 7F) were identified. The Eggerthellaceae family exhibited lower relative abundance with age, regardless of diet or genotype, declining from 0.9 % in 35-week-old mice to 0.6 % in 70-week-old mice ($p < 0.001$, Fig. 7D.i). This family is known for its association with butyrate production and plays a role in generating intermediary urolithins, which have potential anti-inflammatory properties (Selma et al., 2017). Its decline may be both an indicator of, and a contributor togut inflammation. In addition, diet has been suggested to play a role in intestinal microbiota abundance within WT and RAGE KO mice. A dCML-enriched diet led to greater abundance of the Anaerovoracaceae family in RAGE KO mice, irrespective of age (Fig. 7E.i). In WT mice, the Marinifilaceae family was relatively more abundant in the Switch and dCML groups than the STD diet animals ($p <$ 0.001), regardless of age (Fig. 7F.i). Both Anaerovoracaceae and Marinifilaceae families are part of the Bacteroidota phylum (formerly Bacteroidetes), suggesting a shared evolutionary history and functional characteristics. These taxa are known for their roles in glycan metabolism and mucin degradation, processes vital for maintaining intestinal homeostasis and overall gut health (Beaumont et al., 2020; Raimondi et al., 2021). While these slight variations do not decisively explain the differences in inflammatory biomarker expression seen in the Switch group, the fluctuations in minor bacterial taxa could corroborate their distinctive intestinal expression of inflammatory mediators *TNFα* and *IL6* discussed earlier. Taken together, our data the gene expression and microbial communities suggest that minor changes could result from the early-life dietary shift, as evidenced by alterations in the less-abundant taxa outlined above.

The relevant literature highlights the dynamic nature of taxonomic groups in lumen samples, especially in mice exposed to varying levels of dAGEs (van Dongen et al., 2021; Wang et al., 2022; Yuan et al., 2024). This variability includes families such as Akkermansiaceae, Desulfovibrionaceae, Erysipelotriaceae, Lachnospiraceae, and Ruminococcaceae, known for their roles in maintaining intestinal mucus and synthesizing short-chain fatty acids (SCFAs) (Xie et al., 2022; Yan et al., 2022). Their abundance has been reported to increase in response to dAGE intake (Qu et al., 2017; Yuan et al., 2024), but there are conflicting reports of the effect of diet on these groups. Our experimental model did not show significant differences in these families with diet (data not shown), though less abundant families were affected in this regard. Dongen et al. (2021) also described significant variations in microbiota compositions within less abundant families such as Erysepelothrichaceae and Atopobiaceae (van Dongen et al., 2021). Although these taxa exhibited significant correlations with plasma concentrations of dAGEs in mice, they did not show physiological significance concerning the analysed

inflammatory parameters (van Dongen et al., 2021).

It has been reported that colonic bacteria can use glycation products as a carbon source. A study showed that faecal bacteria can degrade at least 40 % of dCML after 24 h of anaerobic incubation (Hellwig et al., 2015). Another recent *in vitro* study on dCML metabolism revealed that nearly 100 % of dCML can be metabolized into carboxymethylated amine derivatives and carboxylic acids (Bui et al., 2019). Through population enrichment assessment, this former study showed that two bacterial groups, *Oscillibacter* and *Cloacibacillus* spp., were found to increase in dCML-enriched media. Under aerobic conditions, up to 66 % of dCML can be degraded, producing bacterial metabolites like N-carboxymethylcadaverine (CM-CAD), N-carboxymethylaminopentanoic acid (CM-APA), and the N-carboxymethyl-1-piperideinium ion (Hellwig et al., 2019). Although the gut microbiota can utilize dietary glycation products and enrich some bacterial species, as demonstrated by Bui and colleagues (2019), our findings suggest that dCML does not preferentially enrich one taxon over any other.

4. Conclusions

To conclude, despite a notable rise in free CML levels across several organs among animals fed a dCML-enriched diet, this increase did not result in observable biological alterations assessed by the biomarkers examined here. Moreover, these findings were observed at doses roughly 13-times higher than the levels of dCML commonly present in laboratory mouse diets and approximately 35-times above the highest concentrations present in human diets (Grossin et al., 2015), indicating a lack of impact even under extreme dosage conditions. We confirmed that dCML tissue accumulation is RAGE independent. The elevated dCML contents in organs and tissue were reversible and did not influence offspring's physiology or gut microbiota. Although minor gene expression changes were noted, particularly in the Switch group which exhibited heightened intestinal sensitivity to inflammation, these changes appear insufficient to have a meaningful impact on overall health. Indeed, our research suggests that age had a more significant impact on the progression of inflammatory gene expression. Our study also shows that over the lifetime of 70 weeks tested here, RAGE deletion had a partial effect in reducing inflammation in animals renal and intestinal tissues. From a pharmaceutical standpoint, our findings underline the importance of inhibiting RAGE as a potential strategy to alleviate the harmful effects of the signalling cascade that results from its activation. This approach has been investigated by various research teams in the last decade (Singh & Agrawal, 2022).

Observed changes in the expression of inflammation biomarkers in the Switch group align with significant nutritional studies showing increased sensitivity of the intestinal tract resulting from early-life diet changes (Differding et al., 2020; Nwaru et al., 2013), but further research is needed to determine the extent to which glycation products play a role in this context. Finally, our findings also accord with previous studies indicating that dAGEs have only a limited impact upon health outcomes, whether over a short or long period of time, and in both animal models (Grossin et al., 2015; Teissier et al., 2019; van Dongen et al., 2021) and humans (Aengevaeren et al., 2023; Berge et al., 2023; Linkens et al., 2022; Linkens et al., 2022). Further research is needed to understand their impact on exacerbating existing pathologies, guiding clinical interventions and dietary recommendations.

In summary, while there were measurable changes in inflammageing biomarkers and gut microbiota composition in response to dietary modifications, these did not translate into significant physiological impacts or health outcomes, highlighting the complexity and resilience of biological systems in their response to dietary changes, and in particular a healthy rodent model to dAGEs.

Funding

This work was funded by Agence Nationale de la Recherche (ANR) [CE34-0013].

CRediT authorship contribution statement

M.T. Nogueira Silva Lima: Writing – review & editing, Writing – original draft, Visualization, Project administration, Methodology, Investigation, Formal analysis, Data curation, Conceptualization. **C. Delayre-Orthez:** Writing – review & editing, Supervision, Project administration, Funding acquisition, Conceptualization. **M. Howsam:** Writing – review & editing, Validation, Supervision, Methodology. **P. Jacolot:** Visualization, Validation, Methodology, Investigation, Formal analysis. **C. Niquet-Léridon:** Visualization, Validation, Methodology, Investigation, Formal analysis. **A. Okwieka:** Validation, Methodology, Investigation, Formal analysis. **P.M. Anton:** Writing – review & editing, Supervision, Methodology, Funding acquisition, Formal analysis, Data curation. **M. Perot:** Writing – review & editing, Visualization, Validation, Methodology, Formal analysis, Data curation. **N. Barbezier:** Supervision. **H. Mathieu:** Formal analysis. **A. Ghinet:** Supervision. **C. Fradin:** Supervision, Investigation. **E. Boulanger:** Supervision, Resources, Project administration, Funding acquisition. **S. Jaisson:** Writing – review & editing, Supervision, Investigation, Funding acquisition, Formal analysis. **P. Gillery:** Writing – review & editing, Validation, Supervision, Project administration, Funding acquisition, Conceptualization. **F.J. Tessier:** Writing – review & editing, Validation, Supervision, Resources, Project administration, Methodology, Funding acquisition, Data curation, Conceptualization.

Declaration of competing interest

The authors declare that they have no known competing financial interests or personal relationships that could have appeared to influence the work reported in this paper.

Data availability

The authors do not have permission to share data.

Appendix A. Supplementary data

Supplementary data to this article can be found online at https://doi.org/10.1016/j.foodres.2024.114967.

References

Aengevaeren, V. L., Berge, K., Mosterd, A., Velthuis, B., Lyngbakken, M. N., Omland, T., Schalkwijk, C., & Eijsvogels, T. M. H. (2023). Advanced glycation endproducts and dicarbonyl compounds are not associated with coronary atherosclerosis characteristics in middle-aged and older male athletes. *European Journal of Preventive Cardiology, 30*(Supplement_1). https://doi.org/10.1093/eurjpc/zwad125.104. zwad125.104.

ALJahdali, N., Gadonna-Widehem, P., Delayre-Orthez, C., Marier, D., Garnier, B., Carbonero, F., & Anton, P. M. (2017). Repeated oral exposure to N ε-carboxymethyllysine, a maillard reaction product, alleviates gut microbiota dysbiosis in colitic mice. *Digestive Diseases and Sciences, 62*(12), 3370–3384. https://doi.org/10.1007/s10620-017-4767-8

Alves-Fernandes, D. K., & Jasiulionis, M. G. (2019). The role of SIRT1 on DNA damage response and epigenetic alterations in cancer. *International Journal of Molecular Sciences, 20*(13), 3153. https://doi.org/10.3390/ijms20133153

Bartling, B., Zunkel, K., Al-Robaiy, S., Dehghani, F., & Simm, A. (2020). Gene doubling increases glyoxalase 1 expression in RAGE knockout mice. *Biochimica et Biophysica Acta (BBA) - General Subjects, 1864*(1), Article 129438. https://doi.org/10.1016/j.bbagen.2019.129438

Beaumont, M., Païs, C., Mussard, E., Knudsen, C., Cauquil, L., Aymard, P., Barilly, C., Gabinaud, B., Zemb, O., Fourre, S., Gautier, R., Lencina, C., Eutamène, H., Theodorou, V., Canlet, C., & Combes, S. (2020). Gut microbiota derived metabolites contribute to intestinal barrier maturation at the suckling-to-weaning transition. *Gut Microbes, 11*(5), 1268–1286. https://doi.org/10.1080/19490976.2020.1747335

Beeri, M. S., Moshier, E., Schmeidler, J., Godbold, J., Uribarri, J., Reddy, S., Sano, M., Grossman, H. T., Cai, W., Vlassara, H., & Silverman, J. M. (2011). Serum concentration of an inflammatory glycotoxin, methylglyoxal, is associated with increased cognitive decline in elderly individuals. *Mechanisms of Ageing and Development, 132*(11–12), 583–587. https://doi.org/10.1016/j.mad.2011.10.007

Berge, K., Aengevaeren, V. L., Mosterd, A., Velthuis, B. K., Lyngbakken, M. N., Omland, T., Schalkwijk, C. G., & Eijsvogels, T. M. (2023). Plasma advanced glycation end products and dicarbonyl compounds are not associated with coronary atherosclerosis in athletes. *Medicine and Science in Sports and Exercise, 55*(7), 1143.

Bodden, C., Hannan, A. J., & Reichelt, A. C. (2020). Diet-induced modification of the sperm epigenome programs metabolism and behavior. *Trends in Endocrinology & Metabolism, 31*(2), 131–149. https://doi.org/10.1016/j.tem.2019.10.005

Boesten, D. M. P. H. J., Elie, A. G. I. M., Drittij-Reijnders, M.-J., den Hartog, G. J. M., & Bast, A. (2014). Effect of Nε-carboxymethyllysine on oxidative stress and the glutathione system in beta cells. *Toxicology Reports, 1*, 973–980. https://doi.org/10.1016/j.toxrep.2014.06.003

Bolyen, E., Rideout, J. R., Dillon, M. R., Bokulich, N. A., Abnet, C. C., Al-Ghalith, G. A., Alexander, H., Alm, E. J., Arumugam, M., Asnicar, F., Bai, Y., Bisanz, J. E., Bittinger, K., Brejnrod, A., Brislawn, C. J., Brown, C. T., Callahan, B. J., Caraballo-Rodríguez, A. M., Chase, J., & Caporaso, J. G. (2019). Reproducible, interactive, scalable and extensible microbiome data science using QIIME 2. *Nature Biotechnology, 37*(8), 852–857. https://doi.org/10.1038/s41587-019-0209-9

Bongarzone, S., Savickas, V., Luzi, F., & Gee, A. D. (2017). Targeting the receptor for advanced glycation endproducts (RAGE): A medicinal chemistry perspective. *Journal of Medicinal Chemistry, 60*(17), 7213–7232. https://doi.org/10.1021/acs.jmedchem.7b00058

Bui, T. P. N., Troise, A. D., Fogliano, V., & de Vos, W. M. (2019). Anaerobic degradation of N-ε-carboxymethyllysine, a major glycation end-product, by human intestinal bacteria. *Journal of Agricultural and Food Chemistry, 67*(23), 6594–6602. https://doi.org/10.1021/acs.jafc.9b02208

Burdet, C., Nguyen, T. T., Duval, X., Ferreira, S., Andremont, A., Guedj, J., & Mentré, F. (2019). Impact of antibiotic gut exposure on the temporal changes in microbiome diversity. *Antimicrobial Agents and Chemotherapy, 63*(10). https://doi.org/10.1128/aac.00820-19

Cai, W., Ramdas, M., Zhu, L., Chen, X., Striker, G. E., & Vlassara, H. (2012). Oral advanced glycation endproducts (AGEs) promote insulin resistance and diabetes by depleting the antioxidant defenses AGE receptor-1 and sirtuin 1. *Proceedings of the National Academy of Sciences, 109*(39), 15888–15893. https://doi.org/10.1073/pnas.1205847109

Cai, W., Uribarri, J., Zhu, L., Chen, X., Swamy, S., Zhao, Z., Grosjean, F., Simonaro, C., Kuchel, G. A., Schnaider-Beeri, M., Woodward, M., Striker, G. E., & Vlassara, H. (2014). Oral glycotoxins are a modifiable cause of dementia and the metabolic syndrome in mice and humans. *Proceedings of the National Academy of Sciences, 111*(13), 4940–4945. https://doi.org/10.1073/pnas.1316013111

Caminero, A., Meisel, M., Jabri, B., & Verdu, E. F. (2019). Mechanisms by which gut microorganisms influence food sensitivities. *Nature reviews. Gastroenterology & hepatology, 16*(1), 7–18. https://doi.org/10.1038/s41575-018-0064-z

Chen, Q., Yan, W., & Duan, E. (2016). Epigenetic inheritance of acquired traits through sperm RNAs and sperm RNA modifications. *Nature Reviews Genetics, 17*(12). https://doi.org/10.1038/nrg.2016.106

Chistiakov, D. A., Sobenin, I. A., Revin, V. V., Orekhov, A. N., & Bobryshev, Y. V. (2014). Mitochondrial aging and age-related dysfunction of mitochondria. *BioMed Research International, 2014*, Article 238463. https://doi.org/10.1155/2014/238463

Constien, R., Forde, A., Liliensiek, B., Gröne, H. J., Nawroth, P., Hämmerling, G., & Arnold, B. (2001). Characterization of a novel EGFP reporter mouse to monitor Cre recombination as demonstrated by a Tie2 Cre mouse line. *Genesis (New York, N.Y.: 2000), 30*(1), 36–44. https://doi.org/10.1002/gene.1030

Dawson, S. L., Mohebbi, M., Craig, J. M., Dawson, P., Clarke, G., Tang, M. L., & Jacka, F. N. (2021). Targeting the perinatal diet to modulate the gut microbiota increases dietary variety and prebiotic and probiotic food intakes : Results from a randomised controlled trial. *Public Health Nutrition, 24*(5), 1129–1141. https://doi.org/10.1017/S1368980020003511

Differding, M. K., Benjamin-Neelon, S. E., Hoyo, C., Østbye, T., & Mueller, N. T. (2020). Timing of complementary feeding is associated with gut microbiota diversity and composition and short chain fatty acid concentrations over the first year of life. *BMC Microbiology, 20*(1), 56. https://doi.org/10.1186/s12866-020-01723-9

Dunkerton, S., & Aiken, C. (2022). Impact of the intrauterine environment on future reproductive and metabolic health. *The Obstetrician & Gynaecologist, 24*(2), 93–100. https://doi.org/10.1111/tog.12797

Dunn, J. A., McCance, D. R., Thorpe, S. R., Lyons, T. J., & Baynes, J. W. (1991). Age-dependent accumulation of N epsilon-(carboxymethyl)lysine and N epsilon-(carboxymethyl)hydroxylysine in human skin collagen. *Biochemistry, 30*(5), 1205–1210. https://doi.org/10.1021/bi00219a007

Ferrucci, L., & Fabbri, E. (2018). Inflammageing : Chronic inflammation in ageing, cardiovascular disease, and frailty. *Nature Reviews. Cardiology, 15*(9), 505–522. https://doi.org/10.1038/s41569-018-0064-2

Fetissov, S. O., & Hökfelt, T. (2019). On the origin of eating disorders : Altered signaling between gut microbiota, adaptive immunity and the brain melanocortin system regulating feeding behavior. *Current Opinion in Pharmacology, 48*, 82–91. https://doi.org/10.1016/j.coph.2019.07.004

Frimat, M., Teissier, T., & Boulanger, E. (2019). Is RAGE the receptor for inflammaging? *Aging, 11*(17), 6620–6621. https://doi.org/10.18632/aging.102256

Gao, S., Quick, C., Guasch-Ferré, M., Zhuo, Z., Hutchinson, J., Su, L., Hu, F., Lin, X., & Christiani, D. (2021). The association between inflammatory and oxidative stress biomarkers and plasma metabolites in a longitudinal study of healthy male welders. *Journal of Inflammation Research, 14*, 2825–2839. https://doi.org/10.2147/JIR.S316262

Gill, P. A., Inniss, S., Kumagai, T., Rahman, F. Z., & Smith, A. M. (2022). The role of diet and gut microbiota in regulating gastrointestinal and inflammatory disease. *Frontiers in Immunology, 13*, Article 866059. https://doi.org/10.3389/fimmu.2022.866059

Gorisse, L., Pietrement, C., Vuiblet, V., Schmelzer, C. E. H., Köhler, M., Duca, L., Debelle, L., Fornès, P., Jaisson, S., & Gillery, P. (2016). Protein carbamylation is a hallmark of aging. *Proceedings of the National Academy of Sciences of the United States of America, 113*(5), 1191–1196. https://doi.org/10.1073/pnas.1517096113

Grossin, N., Auger, F., Niquet-Leridon, C., Durieux, N., Montaigne, D., Schmidt, A. M., Susen, S., Jacolot, P., Beuscart, J.-B., Tessier, F. J., & Boulanger, E. (2015). Dietary CML-enriched protein induces functional arterial aging in a RAGE-dependent manner in mice. *Molecular Nutrition & Food Research, 59*(5), 927–938. https://doi.org/10.1002/mnfr.201400643

Grossin, N., Wautier, M.-P.-S., Picot, J., Stern, D. M., & Wautier, J.-L.-T. (2009). Differential effect of plasma or erythrocyte AGE-ligands of RAGE on expression of transcripts for receptor isoforms. *Diabetes & Metabolism, 35*(5), 410–417. https://doi.org/10.1016/j.diabet.2009.04.009

Hall, B. M., Balan, V., Gleiberman, A. S., Strom, E., Krasnov, P., Virtuoso, L. P., Rydkina, E., Vujcic, S., Balan, K., Gitlin, I. I., Leonova, K. I., Consiglio, C. R., Gollnick, S. O., Chernova, O. B., & Gudkov, A. V. (2017). P16(Ink4a) and senescence-associated β-galactosidase can be induced in macrophages as part of a reversible response to physiological stimuli. *Aging, 9*(8), 1867–1884. https://doi.org/10.18632/aging.101268

Hellwig, M., Auerbach, C., Müller, N., Samuel, P., Kammann, S., Beer, F., Gunzer, F., & Henle, T. (2019). Metabolization of the advanced glycation end product N-ε-carboxymethyllysine (CML) by different probiotic E. coli strains. *Journal of Agricultural and Food Chemistry, 67*(7), 1963–1972. https://doi.org/10.1021/acs.jafc.8b06748

Hellwig, M., Bunzel, D., Huch, M., Franz, C. M. A. P., Kulling, S. E., & Henle, T. (2015). Stability of individual maillard reaction products in the presence of the human colonic microbiota. *Journal of Agricultural and Food Chemistry, 63*(30), 6723–6730. https://doi.org/10.1021/acs.jafc.5b01391

Hellwig, M., Geissler, S., Matthes, R., Peto, A., Silow, C., Brandsch, M., & Henle, T. (2011). Transport of free and peptide-bound glycated amino acids : Synthesis, transepithelial flux at caco-2 cell monolayers, and interaction with apical membrane transport proteins. *Chembiochem, 12*(8), 1270–1279. https://doi.org/10.1002/cbic.201000759

Helou, C., Nogueira Silva Lima, M. T., Niquet-Leridon, C., Jacolot, P., Boulanger, E., Delguste, F., Guilbaud, A., Genin, M., Anton, P. M., Delayre-Orthez, C., Papazian, T., Howsam, M., & Tessier, F. J. (2022). Plasma levels of free NƐ-carboxymethyllysine (CML) after different oral doses of CML in rats and after the intake of different breakfasts in humans : postprandial plasma level of sRAGE in humans. *Nutrients, 14*(9), Article 9. https://doi.org/10.3390/nu14091890

Illien-Jünger, S., Lu, Y., Qureshi, S. A., Hecht, A. C., Cai, W., Vlassara, H., Striker, G. E., & Iatridis, J. C. (2015). Chronic ingestion of advanced glycation end products induces degenerative spinal changes and hypertrophy in aging pre-diabetic mice. *PLoS One1, 10*(2), e0116625.

Ishikawa, S., Matsui, Y., Wachi, S., Yamaguchi, H., Harashima, N., & Harada, M. (2016). Age-associated impairment of antitumor immunity in carcinoma-bearing mice and restoration by oral administration of Lentinula edodes mycelia extract. *Cancer Immunology, Immunotherapy: CII, 65*(8), 961–972. https://doi.org/10.1007/s00262-016-1857-y

Kawai, T., & Akira, S. (2010). The role of pattern-recognition receptors in innate immunity : Update on Toll-like receptors. *Nature Immunology, 11*(5), 373–384. https://doi.org/10.1038/ni.1863

Lee, K.-A., Flores, R. R., Jang, I. H., Saathoff, A., & Robbins, P. D. (2022). Immune senescence, immunosenescence and aging. *Frontiers in Aging, 3*, Article 900028. https://doi.org/10.3389/fragi.2022.900028

Lin, J.-A., Wu, C.-H., Lu, C.-C., Hsia, S.-M., & Yen, G.-C. (2016). Glycative stress from advanced glycation end products (AGEs) and dicarbonyls : An emerging biological factor in cancer onset and progression. *Molecular Nutrition & Food Research, 60*, n/a-n/a. https://doi.org/10.1002/mnfr.201500759

Linkens, A. M. A., Houben, A. J. H. M., Kroon, A. A., Schram, M. T., Berendschot, T. T. J. M., Webers, C. A. B., van Greevenbroek, M., Henry, R. M. A., de Galan, B., Stehouwer, C. D. A., Eussen, S. J. M. P., & Schalkwijk, C. G. (2022). Habitual intake of dietary advanced glycation end products is not associated with generalized microvascular function-the Maastricht Study. *The American Journal of Clinical Nutrition, 115*(2), 444–455. https://doi.org/10.1093/ajcn/nqab302

Linkens, A. M., Houben, A. J., Niessen, P. M., Wijckmans, N. E., de Goei, E. E., Van den Eynde, M. D., Scheijen, J. L., van den Waarenburg, M. P., Mari, A., Berendschot, T. T., Streese, L., Hanssen, H., van Dongen, M. C., van Gool, C. C., Stehouwer, C. D., Eussen, S. J., & Schalkwijk, C. G. (2022). A 4-week high-AGE diet does not impair glucose metabolism and vascular function in obese individuals. *JCI Insight, 7*(6), e156950.

Livak, K. J., & Schmittgen, T. D. (2001). Analysis of relative gene expression data using real-time quantitative PCR and the 2(-Delta Delta C(T)) method. *Methods (San Diego, Calif.), 25*(4), 402–408. https://doi.org/10.1006/meth.2001.1262

Magne, F., Gotteland, M., Gauthier, L., Zazueta, A., Pesoa, S., Navarrete, P., & Balamurugan, R. (2020). The firmicutes/bacteroidetes ratio : A relevant marker of gut dysbiosis in obese patients? *Nutrients, 12*(5). https://doi.org/10.3390/nu12051474

Mallick, H., Rahnavard, A., McIver, L. J., Ma, S., Zhang, Y., Nguyen, L. H., Tickle, T. L., Weingart, G., Ren, B., Schwager, E. H., Chatterjee, S., Thompson, K. N., Wilkinson, J. E., Subramanian, A., Lu, Y., Waldron, L., Paulson, J. N., Franzosa, E. A., Bravo, H. C., & Huttenhower, C. (2021). Multivariable association discovery in population-scale meta-omics studies. *PLOS Computational Biology, 17*(11), e1009442.

Marginã, D., Ungurianu, A., Purdel, C., Tsoukalas, D., Sarandi, E., Thanasoula, M., Tekos, F., Mesnage, R., Kouretas, D., & Tsatsakis, A. (2020). Chronic inflammation in the context of everyday life : Dietary changes as mitigating factors. *International*

Journal of Environmental Research and Public Health, 17(11), 4135. https://doi.org/10.3390/ijerph17114135

Mastrocola, R., Collotta, D., Gaudioso, G., Le Berre, M., Cento, A. S., Ferreira Alves, G., Chiazza, F., Verta, R., Bertocchi, I., Manig, F., Hellwig, M., Fava, F., Cifani, C., Aragno, M., Henle, T., Joshi, L., Tuohy, K., & Collino, M. (2020). Effects of exogenous dietary advanced glycation end products on the cross-talk mechanisms linking microbiota to metabolic inflammation. *Nutrients, 12*(9), Article 9. https://doi.org/10.3390/nu12092497

McMurdie, P. J., & Holmes, S. (2013). phyloseq : An R package for reproducible interactive analysis and graphics of microbiome census data. *PLoS One1, 8*(4), e61217.

Melzer, D., Pilling, L. C., & Ferrucci, L. (2020). The genetics of human ageing. *Nature Reviews Genetics, 21*(2). https://doi.org/10.1038/s41576-019-0183-6. Article 2.

Miró, L., Garcia-Just, A., Amat, C., Polo, J., Moretó, M., & Pérez-Bosque, A. (2017). Dietary animal plasma proteins improve the intestinal immune response in senescent mice. *Nutrients, 9*(12). https://doi.org/10.3390/nu9121346. Article 12.

Mittelbrunn, M., & Kroemer, G. (2021). Hallmarks of T cell aging. *Nature Immunology, 22*(6), Article 6. https://doi.org/10.1038/s41590-021-00927-z

Moretti, I. F., Lerario, A. M., Sola, P. R., Macedo-da-Silva, J., Baptista, M.da. S., Palmisano, G., Oba-Shinjo, S. M., & Marie, S. K. N. (2023). GBM cells exhibit susceptibility to metformin treatment according to TLR4 pathway activation and metabolic and antioxidant status. *Cancers, 15*(3), Article 3. https://doi.org/10.3390/cancers15030587

Negrean, M., Stirban, A., Stratmann, B., Gawlowski, T., Horstmann, T., Götting, C., Kleesiek, K., Mueller-Roesel, M., Koschinsky, T., Uribarri, J., Vlassara, H., & Tschoepe, D. (2007). Effects of low- and high-advanced glycation endproduct meals on macro- and microvascular endothelial function and oxidative stress in patients with type 2 diabetes mellitus. *The American Journal of Clinical Nutrition, 85*(5), 1236–1243. https://doi.org/10.1093/ajcn/85.5.1236

Nogueira Silva Lima, M., Howsam, M., Delayre-Orthez, C., Jacolot, P., Jaisson, S., Criquet, J., Billamboz, M., Ghinet, A., Fradin, C., Boulanger, E., Bray, F., Flament, S., Rolando, C., Gillery, P., Niquet-Léridon, C., & Tessier, F. (2023). Glycated bovine serum albumin for use in feeding trials with animal models – In vitro methodology and characterization of a glycated substrate for modifying feed pellets. *Food Chemistry, 428*, Article 136815. https://doi.org/10.1016/j.foodchem.2023.136815

Nogueira Silva Lima, M. T., Howsam, M., Anton, P. M., Delayre-Orthez, C., & Tessier, F. J. (2021). Effect of advanced glycation end-products and excessive calorie intake on diet-induced chronic low-grade inflammation biomarkers in murine models. *Nutrients, 13*(9). https://doi.org/10.3390/nu13093091. Article 9.

Nwaru, B. I., Takkinen, H.-M., Niemelä, O., Kaila, M., Erkkola, M., Ahonen, S., Haapala, A.-M., Kenward, M. G., Pekkanen, J., Lahesmaa, R., Kere, J., Simell, O., Veijola, R., Ilonen, J., Hyöty, H., Knip, M., & Virtanen, S. M. (2013). Timing of infant feeding in relation to childhood asthma and allergic diseases. *Journal of Allergy and Clinical Immunology, 131*(1), 78–86. https://doi.org/10.1016/j.jaci.2012.10.028

Thornalley, P. J. (2008). Protein and nucleotide damage by glyoxal and methylglyoxal in physiological systems - role in ageing and disease. *Drug Metabolism and Drug Interactions, 23*(1–2), 125–150. https://doi.org/10.1515/DMDI.2008.23.1-2.125

Plunkett, C. H., & Nagler, C. R. (2017). The influence of the microbiome on allergic sensitization to food. *Journal of immunology (Baltimore, Md. : 1950), 198*(2), 581–589. https://doi.org/10.4049/jimmunol.1601266

Qu, W., Yuan, X., Zhao, J., Zhang, Y., Hu, J., Wang, J., & Li, J. (2017). Dietary advanced glycation end products modify gut microbial composition and partially increase colon permeability in rats. *Molecular Nutrition & Food Research, 61*(10). https://doi.org/10.1002/mnfr.201700118

R Core Team. (2022). *R: The R Project for Statistical Computing*. https://www.r-project.org/.

Rabbani, N., & Thornalley, P. J. (2012). Glycation research in amino acids : A place to call home. *Amino Acids, 42*(4), 1087–1096. https://doi.org/10.1007/s00726-010-0782-1

Rabbani, N., & Thornalley, P. J. (2018). Advanced glycation end products in the pathogenesis of chronic kidney disease. *Kidney International, 93*(4), 803–813. https://doi.org/10.1016/j.kint.2017.11.034

Raimondi, S., Musmeci, E., Candeliere, F., Amaretti, A., & Rossi, M. (2021). Identification of mucin degraders of the human gut microbiota. *Scientific Reports, 11*(1), 11094. https://doi.org/10.1038/s41598-021-90553-4

Ratto, D., Roda, E., Romeo, M., Venuti, M. T., Desiderio, A., Lupo, G., Capelli, E., Sandionigi, A., & Rossi, P. (2022). The many ages of microbiome–gut–brain axis. *Nutrients, 14*(14), 2937. https://doi.org/10.3390/nu14142937

Ribeiro, S. A., Braga, E. L. R., Queiroga, M. L., Clementino, M. A., Fonseca, X. M. Q. C., Belém, M. O., Magalhães, L. M. V. C., de Sousa, J. K., de Freitas, T. M., Veras, H. N., de Aquino, C. C., Santos, A. D. C., de Moura, F. R. M., dos Santos, A. A., Havt, A., Maciel, B. L. L., & Lima, A. A. M. (2024). A new murine undernutrition model based on complementary feeding of undernourished children causes damage to the morphofunctional intestinal epithelium barrier. *The Journal of Nutrition*. https://doi.org/10.1016/j.tjnut.2024.02.001

Rojas, A., Schneider, I., Lindner, C., Gonzalez, I., & Morales, M. A. (2022). The RAGE/multiligand axis : A new actor in tumor biology. *Bioscience Reports, 42*(7). BSR20220395.

Sanada, F., Taniyama, Y., Muratsu, J., Otsu, R., Shimizu, H., Rakugi, H., & Morishita, R. (2018). Source of chronic inflammation in aging. *Frontiers in Cardiovascular Medicine, 5*, 12. https://doi.org/10.3389/fcvm.2018.00012

Scheijen, J. L. J. M., Hanssen, N. M. J., van Greevenbroek, M. M., der Kallen, C. J. V., Feskens, E. J. M., Stehouwer, C. D. A., & Schalkwijk, C. G. (2018). Dietary intake of advanced glycation endproducts is associated with higher levels of advanced glycation endproducts in plasma and urine : The CODAM study. *Clinical Nutrition, 37*(3), 919–925. https://doi.org/10.1016/j.clnu.2017.03.019

Šebeková, K., Saavedra, G., Zumpe, C., Somoza, V., Klenovicsová, K., & Birlouez-Aragon, I. (2008). Plasma concentration and urinary excretion of Nε-(Carboxymethyl)lysine in breast milk– and formula-fed infants. *Annals of the New York Academy of Sciences, 1126*(1), 177–180. https://doi.org/10.1196/annals.1433.049

Selma, M. V., Beltrán, D., Luna, M. C., Romo-Vaquero, M., García-Villalba, R., Mira, A., Espín, J. C., & Tomás-Barberán, F. A. (2017). Isolation of human intestinal bacteria capable of producing the bioactive metabolite isourolithin a from ellagic acid. *Frontiers in Microbiology, 8*, 1521. https://doi.org/10.3389/fmicb.2017.01521

Setiawan, B., Budianto, W., Sukarnowati, T. W., Rizky, D., Pangarsa, E. A., Santosa, D., Setiabudy, R. D., & Suharti, C. (2022). Correlation of inflammation and coagulation markers with the incidence of deep vein thrombosis in cancer patients with high risk of thrombosis. *International Journal of General Medicine, 15*, 6215–6226. https://doi.org/10.2147/IJGM.S372038

Singh, H., & Agrawal, D. K. (2022). Therapeutic potential of targeting the receptor for advanced glycation end products (RAGE) by small molecule inhibitors. *Drug Development Research, 83*(6), 1257–1269. https://doi.org/10.1002/ddr.21971

Starowicz, M., & Zieliński, H. (2019). How maillard reaction influences sensorial properties (Color, Flavor and Texture) of food products? *Food Reviews International, 35*(8), 707–725. https://doi.org/10.1080/87559129.2019.1600538

Tamashiro, K. L. K., & Moran, T. H. (2010). Perinatal environment and its influences on metabolic programming of offspring. *Physiology & Behavior, 100*(5), 560–566. https://doi.org/10.1016/j.physbeh.2010.04.008

Tanca, A., Manghina, V., Fraumene, C., Palomba, A., Abbondio, M., Deligios, M., Silverman, M., & Uzzau, S. (2017). Metaproteogenomics reveals taxonomic and functional changes between cecal and fecal microbiota in mouse. *Frontiers in Microbiology, 8*, 391. https://doi.org/10.3389/fmicb.2017.00391

Teissier, T., Boulanger, E., & Cox, L. S. (2022). Interconnections between inflammageing and immunosenescence during ageing. *Cells, 11*(3), 359. https://doi.org/10.3390/cells11030359

Teissier, T., Quersin, V., Gnemmi, V., Daroux, M., Howsam, M., Delguste, F., Lemoine, C., Fradin, C., Schmidt, A.-M., Cauffiez, C., Brousseau, T., Glowacki, F., Tessier, F. J., Boulanger, E., & Frimat, M. (2019). Knockout of receptor for advanced glycation end-products attenuates age-related renal lesions. *Aging Cell, 18*(2), e12850.

Tessier, F. J., Boulanger, E., & Howsam, M. (2021). Metabolic transit of dietary advanced glycation end-products-the case of Nε-carboxymethyllysine. *Glycoconjugate Journal, 38*(3), 311–317.

Tessier, F. J., Niquet-Léridon, C., Jacolot, P., Jouquand, C., Genin, M., Schmidt, A.-M., Grossin, N., & Boulanger, E. (2016). Quantitative assessment of organ distribution of dietary protein-bound 13C-labeled Nε-carboxymethyllysine after a chronic oral exposure in mice. *Molecular Nutrition & Food Research, 60*(11), 2446–2456. https://doi.org/10.1002/mnfr.201600140

Teunisse, G. M. (2022). *Fantaxtic—Nested Bar Plots for Phyloseq Data* (2.0.1) [R]. https://github.com/gmteunisse/Fantaxtic (Édition originale 2018).

The Jackson Laboratory. (2022). *Body Weight Information for Aged C57BL/6J (000664)*. The Jackson Laboratory. https://www.jax.org/jax-mice-and-services/strain-data-sheet-pages/body-weight-chart-aged-b6.

Toda, M., Hellwig, M., Hattori, H., Henle, T., & Vieths, S. (2023). Advanced glycation end products and allergy. *Allergo Journal International, 32*(7), 296–301. https://doi.org/10.1007/s40629-023-00259-4

van Dongen, K. C. W., Kappetein, L., Miro Estruch, I., Belzer, C., Beekmann, K., & Rietjens, I. M. C. M. (2022). Differences in kinetics and dynamics of endogenous versus exogenous advanced glycation end products (AGEs) and their precursors. *Food and Chemical Toxicology, 164*, Article 112987. https://doi.org/10.1016/j.fct.2022.112987

van Dongen, K. C. W., Linkens, A. M. A., Wetzels, S. M. W., Wouters, K., Vanmierlo, T., van de Waarenburg, M. P. H., Scheijen, J. L. J. M., de Vos, W. M., Belzer, C., & Schalkwijk, C. G. (2021). Dietary advanced glycation endproducts (AGEs) increase their concentration in plasma and tissues, result in inflammation and modulate gut microbial composition in mice; evidence for reversibility. *Food Research International, 147*, Article 110547. https://doi.org/10.1016/j.foodres.2021.110547

Vlassara, H., Fuh, H., Makita, Z., Krungkrai, S., Cerami, A., & Bucala, R. (1992). Exogenous advanced glycosylation end products induce complex vascular dysfunction in normal animals : A model for diabetic and aging complications. *Proceedings of the National Academy of Sciences of the United States of America, 89*(24), 12043–12047.

Wang, J., Cai, W., Yu, J., Liu, H., He, S., Zhu, L., & Xu, J. (2022). Dietary advanced glycation end products shift the gut microbiota composition and induce insulin resistance in mice. *Diabetes, Metabolic Syndrome and Obesity, 15*, 427–437. https://doi.org/10.2147/DMSO.S346411

WHO. (2023). *GHE : Life expectancy and healthy life expectancy*. https://www.who.int/data/gho/data/themes/mortality-and-global-health-estimates/ghe-life-expectancy-and-healthy-life-expectancy.

Xie, J., Li, L.-F., Dai, T.-Y., Qi, X., Wang, Y., Zheng, T.-Z., Gao, X.-Y., Zhang, Y.-J., Ai, Y., Ma, L., Chang, S.-L., Luo, F.-X., Tian, Y., & Sheng, J. (2022). Short-chain fatty acids produced by ruminococcaceae mediate α-linolenic acid promote intestinal stem cells proliferation. *Molecular Nutrition & Food Research, 66*(1), e2100408.

Xue, J., Rai, V., Frolov, S., Singer, D., Chabierski, S., Xie, J., Reverdatto, S., Burz, D. S., Schmidt, A. M., Hoffman, R., & Shekhtman, A. (2011). Advanced glycation end product (AGE) recognition by the receptor for AGEs (RAGE). *Structure (London, England : 1993), 19*(5), 722–732. https://doi.org/10.1016/j.str.2011.02.013

Xue, J., Ray, R., Singer, D., Böhme, D., Burz, D. S., Rai, V., Hoffmann, R., & Shekhtman, A. (2014). The receptor for advanced glycation end products (RAGE) specifically recognizes methylglyoxal-derived AGEs. *Biochemistry, 53*(20), 3327–3335.

Yan, J., Pan, Y., Shao, W., Wang, C., Wang, R., He, Y., Zhang, M., Wang, Y., Li, T., Wang, Z., Liu, W., Wang, Z., Sun, X., & Dong, S. (2022). Beneficial effect of the short-chain fatty acid propionate on vascular calcification through intestinal microbiota remodelling. *Microbiome, 10*(1), 195. https://doi.org/10.1186/s40168-022-01390-0

Yousef, H., Czupalla, C. J., Lee, D., Chen, M. B., Burke, A. N., Zera, K. A., Zandstra, J., Berber, E., Lehallier, B., Mathur, V., Nair, R. V., Bonanno, L. N., Yang, A. C., Peterson, T., Hadeiba, H., Merkel, T., Körbelin, J., Schwaninger, M., Buckwalter, M. S., & Wyss-Coray, T. (2019). Aged blood impairs hippocampal neural precursor activity and activates microglia via brain endothelial cell VCAM1. *Nature Medicine, 25*(6). https://doi.org/10.1038/s41591-019-0440-4

Yu, Y., Wang, L., Delguste, F., Durand, A., Guilbaud, A., Rousselin, C., Schmidt, A. M., Tessier, F., Boulanger, E., & Neviere, R. (2017). Advanced glycation end products receptor RAGE controls myocardial dysfunction and oxidative stress in high-fat fed mice by sustaining mitochondrial dynamics and autophagy-lysosome pathway. *Free Radical Biology and Medicine, 112*, 397–410. https://doi.org/10.1016/j.freeradbiomed.2017.08.012

Yuan, X., Liu, J., Nie, C., Ma, Q., Wang, C., Liu, H., Chen, Z., Zhang, M., & Li, J. (2024). Comparative study of the effects of dietary-free and -bound Nε-carboxymethyllysine on gut microbiota and intestinal barrier. *Journal of Agricultural and Food Chemistry, 72*(9), 5014–5025. https://doi.org/10.1021/acs.jafc.3c09395

Zeuke, S., Ulmer, A. J., Kusumoto, S., Katus, H. A., & Heine, H. (2002). TLR4-mediated inflammatory activation of human coronary artery endothelial cells by LPS. *Cardiovascular Research, 56*(1), 126–134. https://doi.org/10.1016/S0008-6363(02)00512-6

Zhong, H., Li, X., Zhou, S., Jiang, P., Liu, X., Ouyang, M., Nie, Y., Chen, X., Zhang, L., Liu, Y., Tao, T., & Tang, J. (2020). Interplay between RAGE and TLR4 regulates HMGB1-induced inflammation by promoting cell surface expression of RAGE and TLR4. *The Journal of Immunology, 205*(3), 767–775. https://doi.org/10.4049/jimmunol.1900860

Zuo, L., Prather, E. R., Stetskiv, M., Garrison, D. E., Meade, J. R., Peace, T. I., & Zhou, T. (2019). Inflammaging and oxidative stress in human diseases: From Molecular mechanisms to novel treatments. *International Journal of Molecular Sciences, 20*(18), 4472. https://doi.org/10.3390/ijms20184472